https://doi.org/10.1016/j.envres.2020.110021

Two decades of trends in urban particulate matter concentrations across Australia

Alma Lorelei de Jesus[a,1], Helen Thompson[b], Luke D. Knibbs[c], Ivan Hanigan[d,2], Lilian De Torres[e], Gavin Fisher[f], Henry Berko[g] and Lidia Morawska[a*]

[a]International Laboratory for Air Quality and Health, Queensland University of Technology, Brisbane, QLD 4000, Australia.
[b]School of Mathematical Sciences, Queensland University of Technology, Brisbane, QLD 4000, Australia. Email: helen.thompson@qut.edu.au
[c]School of Public Health, The University of Queensland, Herston, QLD 4006, Australia. Email: l.knibbs@uq.edu.au
[d]School of Public Health and University Centre for Rural Health, The University of Sydney, Sydney, NSW 2006, Australia. Email: ivan.hanigan@sydney.edu.au
[e]Climate and Atmospheric Science, Science Division, Department of Planning, Industry and Environment, Sydney, NSW 2141, Australia. Email: Lilian.DeTorres@environment.nsw.gov.au
[f]Environment Protection Authority Victoria, Melbourne, VIC 3001, Australia. Email: Gavin.Fisher@epa.vic.gov.au
[g]Environment Division, Department of Environment and Natural Resources, Darwin, NT 0801, Australia. Email: Henry.Berko@nt.gov.au

Also at:
[1]School of Environmental Science and Management, University of the Philippines Los Baños, College, Laguna, 4031, Philippines
[2]Centre for Research and Action in Public Health and Faculty of Health, University of Canberra, Canberra, ACT 2617, Australia

*corresponding author - l.morawska@qut.edu.au

Abstract

Australia is a highly developed country with low population density. Capital cities are situated mainly around the coastline and are subjected to different meteorological conditions. This complex set of drivers is expected to result in varying trends in particulate matter (PM) mass concentrations in urban ambient air across the country. Thus, the aim of this study was to determine the long-term trends in PM_{10} and $PM_{2.5}$ concentrations in capital cities, and to analyse the factors that influenced such trends. The spatial variability of PM concentrations within the capital cities was first established to identify representative stations. Then trends were determined using the Mann-Kendall trend test, Sen's slope, and the generalised additive model. The results show that, in general, the PM concentrations in Australian cities are relatively low (12.1–21.7 $\mu g.m^{-3}$ mean daily PM_{10} and 4.6–8.7 $\mu g.m^{-3}$ mean daily $PM_{2.5}$) and within the WHO daily limit 95% of the time. Over the past two decades, very small declines of 8.0×10^{-5}–1.1×10^{-3} $\mu g.m^{-3}.yr^{-1}$ for PM_{10} and 7.7×10^{-5}–2.6×10^{-3} $\mu g.m^{-3}.yr^{-1}$ for $PM_{2.5}$ were observed while some stations exhibited increase in concentration based on available data; more stations showed a significant monotonic decline for PM_{10} than $PM_{2.5}$. This is attributed to the effectiveness of the implemented emission reduction policies particularly for vehicle exhaust and power generation, given the simultaneous increase in the demand for energy and the number of vehicles over the last two decades. Regarding climate, in the coastal cities of Sydney and Brisbane, high rainfall and strong winds aid in maintaining low PM concentrations despite the significant anthropogenic emissions, while higher PM levels in Darwin can be attributed to its tropical savannah climate, which makes it prone to bushfires and necessitates regular prescribed burnings. PM concentrations increase when exceptional events such as bushfires and dust storms are induced by the extreme climate variability. Further reduction of PM concentrations in Australian cities is unlikely, considering the expanding urbanisation and the changing climate.

Keywords: Australian cities, PM_{10}, $PM_{2.5}$, spatial variability, temporal variability

1. Introduction

Australia is highly developed, has a relatively small population (~25.2 M) and urban centres that are mainly located around the coastline. Australia ranked 3rd in the 2018 Human Development Index (HDI) rank of the United Nations Development Programme (WPR, 2019), which measures the development of a country based on three key dimensions (health, education and standard of living). However, Australia faces challenges that accompany urbanisation and modernisation, such as an increasing population, higher energy demand and air pollution. In general, air quality is much better in Australia than in many other places. However, particulate matter (PM) in the ambient air is at times significant in urban and rural areas of Australia because sources are both natural (e.g. dust and bushfires) and anthropogenic (e.g. industrial, traffic and domestic emissions) (Keywood et al., 2016). Recently, Australia experienced its worst bushfire season, which has been linked to prolonged drought creating the fuel to the fire. Given the vast size of the continent with a diverse range of meteorological conditions, this has a major impact on the fate of pollutants in the air.

In Australia, the National Environment Protection Council (NEPC), created in 1994, established the National Environment Protection (Ambient Air Quality) Measure (AAQ NEPM) in 1998 to regulate air pollution. The AAQ NEPM sets advisory standards (which became quality standards in 2015) for $PM_{2.5}$ (mass concentration of particles with size <2.5 µm) at 25 $\mu g.m^{-3}$ (daily average) and 8 $\mu g.m^{-3}$ (annual average), while the standards for PM_{10} (mass concentration of particles with size <10 µm) are 50 $\mu g.m^{-3}$ (daily average) and 25 $\mu g.m^{-3}$ (annual average). Concurrent with monitoring, control measures and policies for reducing emissions have been established. Among these regulations are the Diesel Vehicle Emissions Measure (2001) and Product Emissions Standards Act (2017) and to ensure continuous improvement of air quality in Australia, the National Clean Air Agreement (2015) was established.

Natural PM sources include resuspended crustal matter from the Outback (remote central Australia) and aged sea salts from the Southern Ocean, which contribute to primary PM (McTainsh et al., 1998; Tadros et al., 2018). Biogenic emissions, particularly from the eucalyptus forests, contribute to secondary PM concentrations, especially in the south east region during the warm and dry season (Emmerson et al., 2016). Additionally, bushfires also occur at this time of the year, and emissions are significant (He et al., 2016; F. H. Johnston et al., 2011; Rea et al., 2016; The Lancet, 2020). In the cooler months, emissions from wood heaters increase PM concentrations (O. Johnston et al., 2016; Jordan et al., 2006) in some areas of Australia. Energy production in Australia has a major impact on the ambient air, as a result of coal mining (Taylor & Isley, 2014) and the use of coal-fired power generation plants (Junkermann & Hacker, 2015). Additionally, various transport systems contribute to PM concentration in the capital cities from motor vehicles, metropolitan railways attributed to non-exhaust particles (Mohsen et al., 2018) and nearby harbours and airports (Broome et al., 2016; Friend & Ayoko, 2009; Mazaheri et al., 2011).

Meteorology (in particular, wind speed and direction, precipitation and ambient temperature) and landscapes (which greatly influence the natural dispersion and dilution process), are inherent to a place and are critical factors in affecting air pollution. Different climate types are experienced by the eight states and mainland territories of Australia. The biophysical features of the whole country's landscape also vary (Hutchinson et al., 2005). According to the Köppen-Geiger climate classification system, Darwin has a tropical savannah climate (Aw); Sydney and Brisbane both have a humid subtropical climate (Cfa); Melbourne, Canberra, and Hobart have an oceanic climate (Cfb); and Perth and Adelaide have a hot-summer Mediterranean climate (Csa). Darwin has distinct wet (November to April) and dry (May to October) seasons of the tropical region contrary to the winter (June to August), spring (September to November), summer (December to February) and autumn (March to May) of the temperate region. Temperate regions experience great variations in rainfall and wind because of the temperature difference between the tropics and the polar zones.

Given the complex interplay of the factors driving PM concentrations in cities (such as emission sources, regulations and meteorological conditions), understanding which factor contribute to mass concentrations of PM across Australia can provide insights to future trends and pointers for effective mitigation. Therefore, this study examined: (1) long-term trends in PM_{10} and $PM_{2.5}$ among Australian capital cities; and (2) factors causing the variability and changes. However, we did not intend to analyse each driver separately due to complications. For example, the bushfire smoke is a major complicating factor since impacts are wide range. Thus, acknowledging that identifying the individual impacts of these factors is beyond the scope of this study.

2. Materials and methods

This study included all capital cities in the eight states and territories of Australia, namely Adelaide, Brisbane, Canberra, Darwin, Hobart, Melbourne, Perth, and Sydney. The boundary considered for each capital city was that of the greater capital city as defined by the Australian Bureau of Statistics, representing the socio-economic extent. The greater capital city boundary was considered to delimit the study areas since it includes the urban area of the city, which covers most of the commuting population. The selection criteria for the monitoring stations of the capital cities were: (1) it should have collected both PM_{10} and $PM_{2.5}$ concurrently; (2) it should have measured concentrations in a daily resolution or higher; and at least 6 months of data should be available per year. AS/NZS 3580.1.1 provides a guide on the selection and siting criteria of monitoring stations. Stations designated as urban background (UB) are sited in areas with homogenous land use and geography and are located 50 m from the road to assess transportation of pollution in the region. Stations classified as roadside (RS), also called peak sites, are located at least 2 m from the road and are important for source emission monitoring. Both types represent the urban ambient concentrations of particulate matter.

2.1 Instrumentation

Measurements of ambient PM concentrations in all cities were either through the gravimetric method using the tapered element oscillating microbalance (TEOM) or by beta attenuation monitoring (BAM). These instruments are considered as US EPA federal equivalent methods (FEM) for PM concentration measurements. In an oscillating microbalance analyser, the particle mass is proportional to the magnitude of the frequency change while in a beta gauge, it is proportional to the difference between the baseline beta and the beta count after sampling. Both techniques comply with AS/NZS 3580 for the standard methods for sampling and analysis of ambient air (i.e. AS/NZS 3580.9.7, AS 3580.9.8, AS/NZS 3580.9.11, AS/NZS 3580.9.12, AS/NZS 3580.9.13, and AS/NZS 3580. 9.16). Earlier data collected using TEOMs (both PM_{10} and $PM_{2.5}$) were adjusted using an empirical USEPA PM_{10} equivalency correction factor of 1.03x + 3.00. However, it was soon realised that the factor was not appropriate for Australian conditions; it either under-estimates the concentration like in Hobart (Innis et al., 2013) or it over-estimates the concentration like in Darwin (CSIRO, 2001). Thus, the use of this equivalency correction factor varied among the Australian cities; Sydney and Brisbane no longer apply this for their $PM_{2.5}$ while Perth continued to use it. Moreover, newer models of TEOMs can effectively address the loss of semi-volatile components from the collected particulate matter with the filter dynamic measurement system.

Given the variation in the data collection process across Australia over the study period, data were used as provided. Further, since the focus of this study was on the trend, the magnitude of individual measurements was less critical. Comparison of concentrations among the cities is therefore limited to the results obtained from the available data.

2.2 Data analysis

Daily resolution for the particulate matter mass concentrations was chosen to capture the short-term fluctuations in analysing the trend. All data were used in the form provided by the different institutions. Some datasets provided had already undergone strict quality control measures based on the AS/NZS mentioned earlier. Some were given as raw instrument readings, in which case, data quality was checked based on the recorded status code and operating conditions of the instrument, and then invalid measurements (e.g. extremely negative values) were removed prior to averaging. The daily concentrations were calculated if at least 50% of hourly measurements were available. All data were analysed using R software (RStudio Team, 2016).

2.2.1 PM_{10} and $PM_{2.5}$ general trends

The variability and trends of PM_{10} and $PM_{2.5}$ concentrations in the capital cities were determined by analysing the long-term daily measurements from the selected stations. A boxplot was prepared to visualise the concentrations among the stations. Then, the ratio of the daily PM_{10} and $PM_{2.5}$ was computed and was presented in a boxplot. A higher $PM_{2.5}/PM_{10}$ suggests larger contribution from anthropogenic sources (e.g. combustion sources), while a lower ratio indicates a significant contribution from natural sources (e.g. crustal matter) (Sugimoto et al., 2016).

2.2.2 Variability of PM concentrations

The spatial variability of the PM_{10} and $PM_{2.5}$ concentrations within cities was tested using Pearson's correlation coefficient (*r*) and the coefficient of divergence (COD) among paired sites within a city (Massoud et al., 2011; Qadir et al., 2014; Yadav & Turner, 2014). Pearson's *r* provides a measure of the linear relationship between two variables; thus, in this case, a high correlation between site pairs suggests that the sites share similar sources. The COD, on the other hand, describes the intra-urban concentration heterogeneity; a heterogeneity greater than 20% (COD > 0.2) indicates variations among sites. Time series plots were also prepared to illustrate daily variability in PM concentrations. Linear trends were then obtained using the two-sided Mann-Kendall (MK) trend test, which determines if the data follow a monotonic trend, and the Sen's slope, which gives the magnitude of the trend (Masiol et al., 2018; Pandolfi et al., 2016). The *mk.test* and *sens.slope*, both from the *trend* package (Pohlert, 2018) were used for the trend analysis. The *tsclean* function from the *forecast* package (Hyndman et al., 2018) was used to impute missing values.

One station was selected to represent each capital city based on the *r* and COD values, then similarities and differences in the PM_{10} and $PM_{2.5}$ concentrations among the cities were analysed. The seasonality and the changes in concentration over time of PM_{10} and $PM_{2.5}$ in the capital cities were studied. The number of exceedances in the daily PM_{10} and $PM_{2.5}$ concentrations against the NEPM standards was also investigated. The generalised additive model (GAM) using the *stat_smooth* function of the *ggplot2* package (Wickham, 2009) was applied to obtain the seasonal and long-term pattern. GAM uses a smoothing function such as splines instead of a linear predictor to obtain a fitted line. There are various methods that can be used to obtain trends but given the multitude of factors influencing PM concentrations and the uncertainty in cyclical patterns, the use of GAM, which does not require regularly spaced pattern, is appropriate. Changes were explained with respect to main urban sources, such as progress in transportation and fuel technology as well as climatic conditions in the cities. Meteorological records and data for all Australian states were obtained from the Bureau of Meteorology (BOM) of Australia.

2.2.3 Relationship of PM_{10} and $PM_{2.5}$ among cities

The correlation of PM_{10} or $PM_{2.5}$ between cities was determined using the *cor* and *cor.test* functions of the *stats* package (R Core Team, 2018) to compute the correlation matrix then the *order.single* function of the *gclus* package (Hurley, 2019) was applied, which orders the objects using hierarchical clustering and the *cpairs* function, which creates the scatterplot matrix. Only days with complete observations for all cities were used for the paired correlation test. Then, the principal components and cluster analyses (Dogruparmak et al., 2014) were performed using the same data matrix. Principal components and cluster analyses reduce the complexity of observed data by identifying the minimum number of significant underlying dimensions to explain the observed data, and then group the variables forming fewer and more homogenous sets. The *prcomp* function of the *stats* package was used to perform the principal components analysis. Then the eigenvalues (i.e. based on Guttman-Kaiser criterion, eigenvalues > 1) and cumulative proportions of the variance were evaluated to identify the number of significant components. As a confirmatory step, the number of components identified by the principal component analysis was tested after applying the varimax rotation technique using the *principal* function of the *psych* package (Revelle, 2019). The loading matrix was rotated to achieve the simplest structure; varimax does this by maximising the variance of the squared loadings of the factor (column) on all the variables (row) in a matrix. The *principal* function decomposes the eigenvalues of the correlation matrix, and then determines the degree of fit for the specified number of components.

After identifying the number of significant components, fuzzy c-means clustering was performed using the *fcm* function of the *ppclust* package (Cebeci et al., 2019) to determine the possible clusters for the Australian capital cities (i.e. data points in the same cluster have similar properties). Unlike partition clustering (e.g. k-means), fuzzy clustering does not classify an object into only one cluster. Thus, outliers are not forced to belong to a particular cluster; rather they are assigned with membership probability. The Dunn's fuzziness coefficient and the ratio of the "between sum of squares" and "total sum of squares" (BSS/TSS) were used to measure the goodness of the clustering, which should approach 1 meaning high likelihood of belonging to the cluster. The obtained clusters were then evaluated and the factors that caused such clustering were identified.

3. Results and discussion

The daily PM_{10} and $PM_{2.5}$ from 23 monitoring stations across Australia were analysed. The stations in each capital city used in this study are listed in Table 1, and detailed descriptions are provided in the supplementary material (Table S1 and Figure S1). There is only one station representing Hobart (HBA1), since HBA2 (Launceston) is in another city, also in the state of Tasmania. Among the cities under study, Sydney had the longest monitoring record for PM_{10} (25 years; 1993 – 2017), while Perth had the longest record for $PM_{2.5}$ (1994 – 2017). Canberra, on the other hand, had the shortest record of at least two years for both metrics. Although the available data for the capital cities have different duration, we opted to use them for the analysis while noting it as a limitation but still addressing the aims of our study. The sample size per station per metric (PM_{10} or $PM_{2.5}$) is also presented in Table 1. The available data for the period covered were more than 80% for all stations except for BNE4 (79% for PM_{10} and 71% for $PM_{2.5}$) and CBR1 (76% for $PM_{2.5}$). Most stations are sited in residential areas, commonly in proximity to a commercial and/or light industrial area.

3.1 PM_{10} and $PM_{2.5}$ concentrations in cities

Figure 1 presents the boxplots of the daily PM_{10} and $PM_{2.5}$ concentrations for all the monitoring stations. The mean daily PM_{10} ranged from 10.0 to 20.2 $\mu g.m^{-3}$ and the mean $PM_{2.5}$ ranged from 4.6 to 8.7 $\mu g.m^{-3}$ for the UB stations. Among the cities, Darwin had the highest mean PM_{10} and $PM_{2.5}$ concentrations at DRW1 while Canberra had the lowest mean PM_{10} at CBR3 and Hobart had the lowest mean $PM_{2.5}$ concentrations at HBA1. The two stations in Darwin had the widest interquartile range and the highest 95th percentile. In contrast, the Hobart and Adelaide stations had narrowest interquartile range while the

Canberra and Adelaide stations had the lowest 95th percentiles for PM_{10} and $PM_{2.5}$, respectively. HBA1 and HBA2 measurements did not differ much (i.e. mean difference of 2.1 $\mu g.m^{-3}$ for PM_{10} and 1.1 $\mu g.m^{-3}$ for $PM_{2.5}$) given that they are located in different cities. It can also be observed from the boxplots that a high PM_{10} does not necessarily correspond to a high $PM_{2.5}$ and vice versa, as seen in Adelaide, Darwin, and Melbourne.

Table 1. The monitoring stations within the boundary of the Greater Capital City selected for the study.

City/Stations	Code	Coordinates	*Type	Period Covered		Sample size (n)		Institution
				PM_{10}	$PM_{2.5}$	PM_{10}	$PM_{2.5}$	
Adelaide, South Australia (SA)								
Adelaide CBD	ADL1	34.9289°S, 138.6010°E	UB	2014 – 2017	2014 – 2017	1363	1361	Environment Protection Authority South Australia
Le Fevre 2	ADL2	34.7913°S, 138.4979°E	UB	2013 – 2017	2013 – 2017	1653	1704	
Netley	ADL3	34.9438°S, 138.5491°E	UB	2005 – 2017	2005 – 2017	4616	4687	
Brisbane, Queensland (QLD)								
Rocklea	BNE1	27.5358°S, 152.9934°E	UB	1996 – 2017	1998 – 2017	7237	6538	Department of Environment and Science
South Brisbane	BNE2	27.4848°S, 153.0321°E	RS	2001 – 2017	2009 - 2017	5724	3094	
Springwood	BNE3	27.6125°S, 153.1356°E	UB	1999 – 2017	1999 – 2017	6708	6726	
Woolloongabba	BNE4	27.4975°S, 153.0350°E	RS	1998 – 2017	2008 – 2017	5781	2607	
Canberra, Australian Capital Territory (ACT)								
Civic	CBR1	35.2853°S, 149.1316°E	RS	2012 – 2016	2015 – 2016	1801	555	Australian Capital Territory Health
Florey	CBR2	35.2206°S, 149.0435°E	UB	2014 – 2016	2014 – 2016	1028	1002	
Monash	CBR3	35.4183°S, 149.0940°E	UB	2012 – 2016	2013 – 2016	1815	1287	
Darwin, Northern Territory (NT)								
Palmerston	DRW1	12.5078°S, 130.9485°E	UB	2011 – 2017	2011 – 2017	2218	2218	Northern Territory Environment Protection Authority
Winnellie	DRW2	12.4243°S, 130.8934°E	UB	2012 – 2017	2012 – 2017	1792	1792	
Hobart, Tasmania (TAS)								
Hobart	HBA1	42.8546°S, 147.3151°E	UB	2009 – 2017	2010 – 2017	3198	2642	Department of Primary Industries, Parks, Water and Environment
Launceston	HBA2	41.4177°S, 147.1249°E	UB	2010 – 2017	2011 – 2017	2676	2434	
Melbourne, Victoria (VIC)								
Alphington	MEL1	37.7783°S, 145.0306°E	UB	1995 – 2017	2014 – 2017	8060	1264	Environment Protection Authority Victoria
Footscray	MEL2	37.8048°S, 144.8727°E	UB	1997 – 2017	2015 – 2017	7273	947	
Perth, Western Australia (WA)								
Caversham	PER1	31.8758°S, 115.9774°E	UB	2004 – 2017	1994 – 2017	5049	7736	Department of Water and Environmental Regulation
Duncraig	PER2	31.8264°S, 115.7829°E	UB	1997 – 2017	1995 – 2017	7416	8223	
South Lake	PER3	32.1106°S, 115.8348°E	UB	2000 – 2017	2006 – 2017	6470	4280	
Sydney, New South Wales (NSW)								
Chullora	SYD1	33.8939°S, 151.0453°E	UB	2003 – 2017	2003 – 2017	5387	5297	Department of Planning, Industry and Environment
Earlwood	SYD2	33.9178°S, 151.1347°E	UB	1995 – 2017	1997 – 2017	7893	7432	
Liverpool	SYD3	33.9328°S, 150.9058°E	UB	1993 – 2017	1998 – 2017	8487	6942	
Richmond	SYD4	33.6183°S, 150.7458°E	UB	1994 – 2017	1996 – 2017	8519	7359	

*monitoring station type is either urban background (UB) or roadside (RS)

Note: Only Adelaide, Brisbane, Melbourne, and Sydney have other stations located within the greater capital city area aside from the selected ones. However, those stations have lesser $PM_{2.5}$ data.

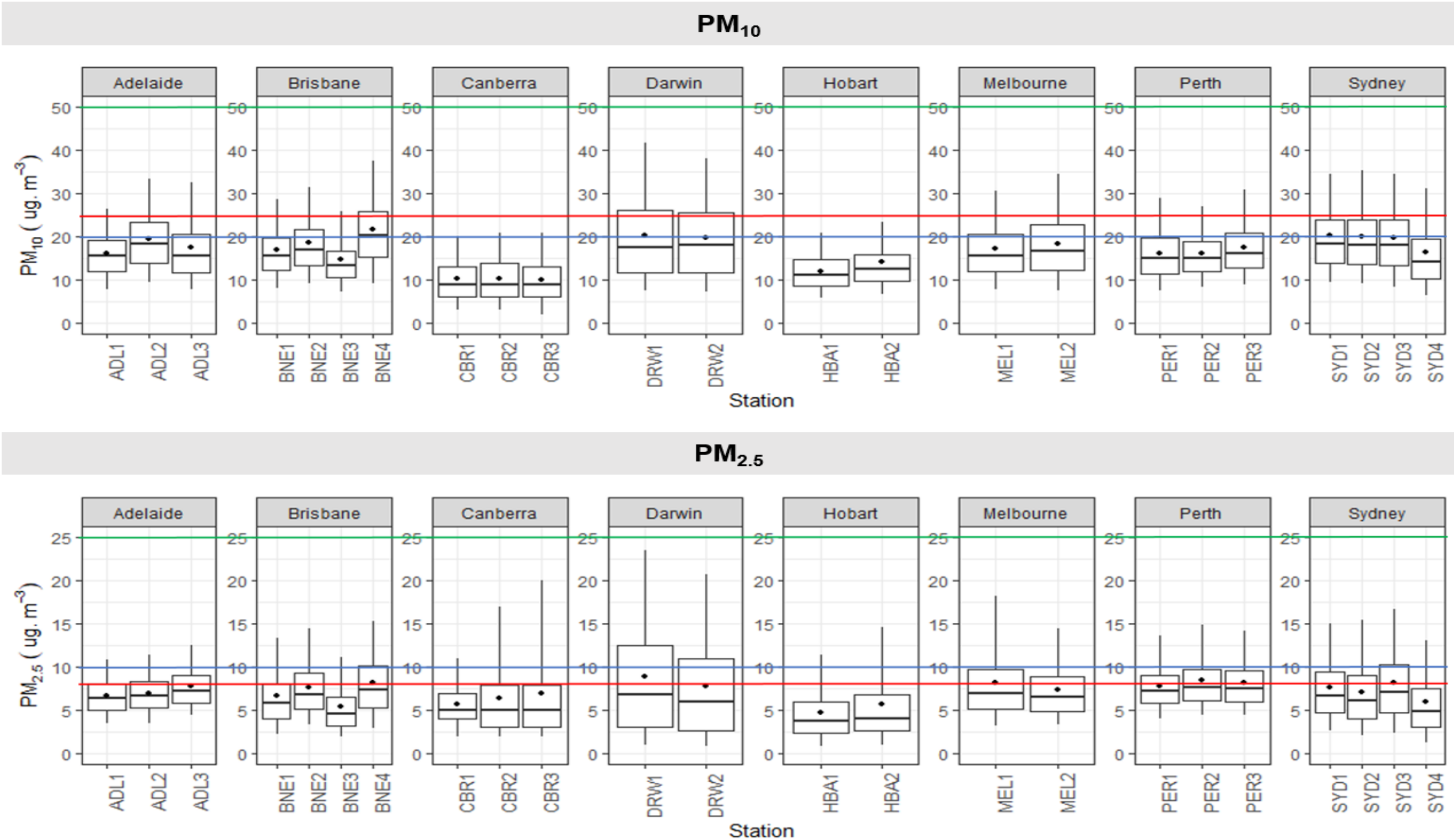

Figure 1. Boxplot for the daily PM_{10} and $PM_{2.5}$ concentrations in the different monitoring stations with the mean, median, the interquartile range (IQR), the 5th percentile, and the 95th percentile. Green line corresponds to the daily average standard of the National Environment Protection Measure (NEPM) and WHO guideline values, red line for annual average NEPM standard and blue line for annual average WHO guideline values.

The mean concentrations of both PM_{10} and $PM_{2.5}$ concentrations and even the 95th percentile (the top of the whiskers) were below the NEPM standard values of 50 µg.m^{-3} and 25 µg.m^{-3} for the daily averages, respectively. These standards are the same as the WHO's guideline values for daily averages. However, in considering the standards for annual averages, the mean concentrations in some stations exceeded the 8 µg.m^{-3} the annual average NEPM standard for $PM_{2.5}$, such as these UB sites DRW1 (8.7 µg.m^{-3}), PER2 (8.4 µg.m^{-3}), MEL1, PER3 and SYD3 (8.2 µg.m^{-3}) and RS site BNE4 (8.2 µg.m^{-3}). However, these stations still meet the 25 µg.m^{-3} annual average NEPM standard for PM_{10}. In contrast, if comparing with the WHO guideline values for annual averages, the $PM_{2.5}$ in the Australian cities complied with the 10 µg.m^{-3} value, but not with the 20 µg.m^{-3} for PM_{10}. The PM_{10} for UB sites DRW1 and SYD1 was 20.2 µg.m^{-3}, while BNE4 measured 21.7 µg.m^{-3}. All median concentrations were within the NEPM standards and WHO guideline values for both daily and annual averages except for the PM_{10} at BNE4 (20.3 µg.m^{-3}).

In most urban areas, sources are dominated by vehicular emissions and domestic fuel burning, and are thus highly correlated with population (Li et al., 2017; Sharma et al., 2014). Figure S2 presents the population growth in the capital cities, motor vehicle count registrations and fuel consumption data per state and territory according to the Australian Bureau of Statistics. Among the capital cities, Greater Sydney has the highest population percentage (20.9%), while Greater Darwin has the lowest (0.6%) of the 25.2 million people in Australia. There were 19.2 million registered vehicles in Australia as of January 2018, and the number of registered vehicles has increased in all states and territories. Passenger vehicles comprise 74.7% of all registered vehicles in Australia, but light rigid trucks have the highest growth rate. Petrol-powered vehicles constitute 74.6%, while diesel-powered vehicles make up 23.4% of the national fleet and are still the fastest growing fuel type. The Northern Territory has the lowest number of registered vehicles followed by the ACT, Tasmania, Queensland, Victoria, and NSW with the highest number.

Based on the presented PM concentrations, population, and vehicle counts, the correlation between anthropogenic emissions and PM concentrations was not strictly followed by all capital cities in Australia. For example, Darwin, with the lowest population (~150,000 as of 2018) and vehicle count had the highest PM concentrations therefore other local sources persist. However, the low PM concentrations in Canberra and Hobart were expected due to the low population and low number of vehicles, while the high population and high number of vehicles in Sydney, Melbourne, and Brisbane were reflected in the high PM concentrations. The effect of vehicle emissions is clearly seen in the high PM concentrations recorded at the RS sites in Brisbane (BNE2 and BNE4). The difference in concentrations between BNE2 and BNE4 can be explained by their proximity to a major road. In contrast, MEL2 had lower $PM_{2.5}$ since it is sited within the Hansen Reserve (i.e. a large open space with playground and multiple sports fields), although it had a considerably higher PM_{10}. SYD4 had lower PM concentrations than the other three monitoring stations since the area is semi-rural.

Aside from traffic (i.e. tail pipe and non-exhaust) as an emission source affecting cities, industrial emissions and activities in harbours and airports influence PM concentrations. In Queensland, emissions from a coal-fired power plant have been proven to contribute to ambient particulate matter (Junkermann & Hacker, 2015) with three plants relatively close to the Brisbane central business district (Tarong, 135 km NW, producing 1415 MW; Millmeran, 190 km SSW, producing 852 MW; and Kogan Creek, 235 km WNW, producing 744 MW) (DNRME, 2019). HBA2 (Launceston), located on the banks of the Tamar River, may occasionally be affected by the heavy industrial area at Bell Bay under unfavourable conditions. Further, the contribution of these sources can be observed in the variation of PM_{10} and $PM_{2.5}$ in Adelaide and Darwin as mentioned earlier. ADL2 is located on the Le Fevre Peninsula where a cement manufacturing plant operates; therefore, higher PM_{10} was observed. ADL3, on the other hand, is sited directly opposite the Adelaide airport that probably contributes to $PM_{2.5}$ concentrations. In Darwin, the PM_{10} concentrations were comparable between DRW1 and DRW2, but the $PM_{2.5}$ concentrations were not. DRW1 was set-up to monitor airborne pollutants that enter the central business district from the Middle Harbour, a vital transportation hub for northern Australia. Therefore, the elevated $PM_{2.5}$ level in DRW1 is greatly influenced by Harbour activities. DRW2, on the other hand, is located in a residential/light industrial area of the Northern Territory.

3.2 PM characteristics in Australian cities

PM_{10} particles include crustal matter, sea salts, non-exhaust emissions (e.g. resuspended road dust and wear from tyres, brakes, and clutches), and mechanically formed particles, while $PM_{2.5}$ particles are derived mostly from combustion processes (e.g. tail-pipe emissions, bushfire smoke and energy production) and new particle formation (NPF). Thus, a higher $PM_{2.5}/PM_{10}$ ratio suggests a major contribution from $PM_{2.5}$ sources. The median $PM_{2.5}/PM_{10}$ ratio ranged from 0.32 – 0.62, with the lowest values in Hobart and the highest values in Canberra (Figure 2). These values indicate that particulate matter in Hobart is mostly derived from natural sources, while that of Canberra originates largely from human activities. However, if the $PM_{2.5}/PM_{10}$ ratio is calculated for the entire year, the value is generally higher due to increased emissions of $PM_{2.5}$ in particular seasons (Shahsavani et al., 2012). In the case of Hobart, increased emissions are generated by the use of wood heaters during the cold season while Canberra is also affected by emissions from vegetation burning during the dry season and wood heaters, and occasionally by dust storms carried by the westerly winds.

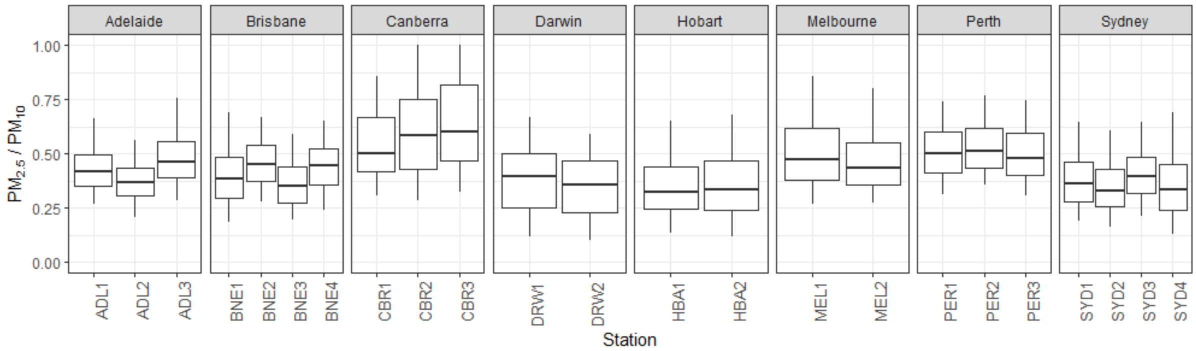

Figure 2. $PM_{2.5}/PM_{10}$ ratio for each station in the different capital cities.

Non-dust particles such as sea salts and coarse-mode nitrate (i.e. sea salt particles that have reacted with nitric acid) can give false signals causing higher PM_{10} (Sugimoto et al., 2016); being the only city not on the coastline, the high ratio of Canberra has demonstrated this. Additionally, the observed $PM_{2.5}/PM_{10}$ values that correspond to non-dust aerosols ranged from 0.7 to 0.8, while those of local and transported dust were <0.3. Zhao et al. (2019) validated how the degree of change in the $PM_{2.5}/PM_{10}$ ratio is directly affected by the relatively variable $PM_{2.5}$, which comes from sources that are more diverse and is easily influenced by various factors. However, it should be noted that the stations within each city had relatively small differences in the ratio, which we consider to be due to similar emission sources and diffusion conditions. A better understanding of this $PM_{2.5}/PM_{10}$ ratio through analysis of diurnal and seasonal variations is recommended to aid in control and management.

3.3 Spatial variability within cities

The general trends in PM concentrations and characteristics presented have already revealed some similarities and differences among the stations. Based on Pearson's r of the pairwise analysis, the PM_{10} are well-correlated ($0.69 \leq r \leq 0.98$) within cities and as expected, HBA1 and HBA2 (r = 0.14) are not (Figure S3). HBA1 (Hobart) and HBA2 (Launceston) are 198 km apart, with Launceston being located in the Tamar Valley while Hobart is coastal, and therefore having different atmospheric conditions affecting particle diffusion and the impact of wood heaters in cold months (Mészaros et al., 2015). The stations have a lower Pearson's r ($0.62 \leq r \leq 0.89$) for $PM_{2.5}$ than for PM_{10} measurements

(Figure S4) suggesting that $PM_{2.5}$ sources are more localised, with proximity to the station as a factor. For example, the Pearson's *r* for $PM_{2.5}$ in Hobart was 0.30, higher than the PM_{10}. Darwin also had a higher Pearson's *r* for $PM_{2.5}$ confirming that for these two cities, the PM_{10} concentrations are very varied. The COD values further support the correlation test (Figures S3 and S4), showing that PM_{10} is more homogenous (COD < 0.20) while $PM_{2.5}$ tends to be more heterogeneous in most cities except Adelaide, Melbourne and Perth. These three cities also have low COD values (~0.1) for PM_{10}, indicating that particulate matter in the airshed is consistent.

3.4 Temporal variability among cities

According to Sen's slope of the daily mass concentrations, the PM_{10} in the capital cities has declined, although the rate was relatively small. However, $PM_{2.5}$ has shown much more complexity in trends. In the MK trend test, a negative monotonic trend in daily PM_{10} was detected for most stations, while a mixed result for the trend test was observed for daily $PM_{2.5}$; half of the stations had no monotonic trend, while the other half was split into either positive or negative monotonic trends. The decrease in PM_{10} ranged from 8.0×10^{-5} $\mu g.m^{-3}.yr^{-1}$ (SYD2) to 1.1×10^{-3} $\mu g.m^{-3}.yr^{-1}$ (ADL2 and BNE4). The daily PM_{10} concentrations for CBR2, CBR3, HBA2, and SYD3 remained the same (slope = 0) while ADL1, CBR1, and DRW2 increased (7.0, 8.4 and 6.8×10^{-4} $\mu g.m^{-3}.yr^{-1}$, respectively). BNE1, BNE2, CBR1, DRW2, and HBA2 experienced an increase in $PM_{2.5}$, while ADL3, CBR2, PER1, PER3, and SYD1 had a zero slope. The decreases in $PM_{2.5}$ (7.7×10^{-5} to 2.6×10^{-3} $\mu g.m^{-3}.yr^{-1}$) and PM_{10} are comparable in magnitude. All stations within the cities exhibited variability in trends except for the Melbourne stations, which consistently showed a decline in concentration, although PM_{10} had a monotonic trend while $PM_{2.5}$ had none.

3.4.1 Daily variations

Day-to-day variations in the PM_{10} and $PM_{2.5}$ concentrations can be observed from the time series plots (Figure S5 and S6). Some extreme elevated concentrations were recorded in Brisbane and Sydney in September 2009 (i.e. PM_{10} concentrations > 1000 $\mu g.m^{-3}$ and $PM_{2.5}$ concentrations > 200 $\mu g.m^{-3}$); a dust storm that lasted for several days blew crustal matter from the Lake Eyre Basin (1600 km W of Brisbane and 1500 NW of Sydney) as a result of severely dry conditions (Aryal et al., 2015). ADL3, BNE1, CBR3, DRW2, HBA1, MEL1, PER2 and SYD2 were selected to represent the cities in which they are located. These stations were the least affected by localised sources based on the above analysis. The daily exceedance of the corresponding AAQ NEPM standards, one measure used by the states and territories to characterise the ambient air quality was plotted (Figure 3). High

PM_{10} mostly occurred in 2009, and then fewer days with concentrations higher than 50 µg.m^{-3} were experienced after that. In contrast, the exceedances for $PM_{2.5}$ (concentrations > 25 µg.m^{-3}) were mostly recorded after 2012, with the highest number of exceeding days in 2015. However, these results may not be completely reflective of the actual conditions since some capital cities have no data earlier than 2012 for PM_{10} and 2014 for $PM_{2.5}$. The exceedances in all cities are recorded in their annual NEPM compliance report, and causes of extreme PM concentrations are usually bushfires, both wildfires and planned burns. It can also be observed that an exceedance in PM_{10} does not always correspond to an exceedance in $PM_{2.5}$ and vice versa.

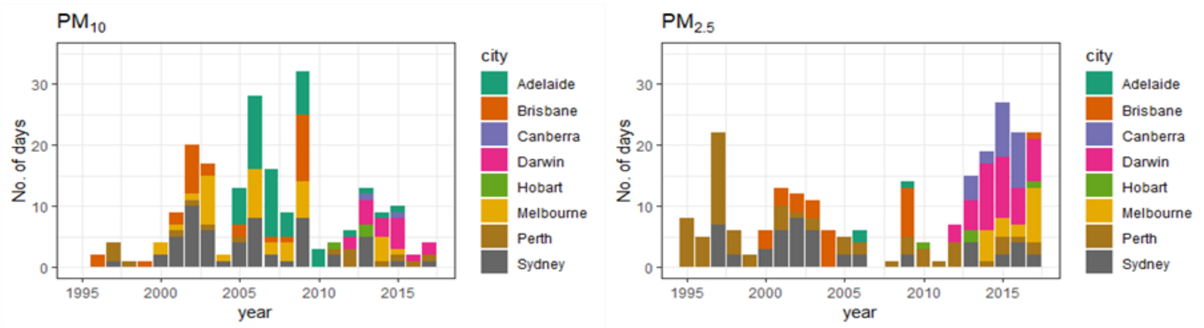

Figure 3. Daily PM_{10} and $PM_{2.5}$ exceedances against the NEPM standards per year per city.

3.4.2 Seasonal variations

The seasonal trends obtained by GAM further showed that the PM_{10} and $PM_{2.5}$ among capital cities varied (Figure 4). Darwin had a very distinct pattern for both particulate matter mass concentrations; a sudden increase in concentration started in April, the peak concentration occurred in July, then a decrease until December. Canberra, Hobart, and Melbourne had similar patterns for PM_{10}, high concentrations around April and May, then low concentrations around August, although the magnitude of changes in concentrations was different. The $PM_{2.5}$ of these three cities were also the same, concentrations start increasing in March, peaking around June then become low and stable from August. The $PM_{2.5}$ peak in Canberra winter is believed to be due to wood heater smoke. Adelaide and Perth had comparable PM_{10} and $PM_{2.5}$ seasonal trends; high PM_{10} concentrations around January and February, then low concentrations in June and July. Their $PM_{2.5}$, on the other hand, was high during these months. The seasonal trends for PM_{10} in Brisbane and Sydney were alike, with peak concentrations in September. The $PM_{2.5}$ had the opposite patterns; Brisbane's $PM_{2.5}$ matched its PM_{10} trend, while Sydney's $PM_{2.5}$ was high around May and June, but concentrations decreased towards September.

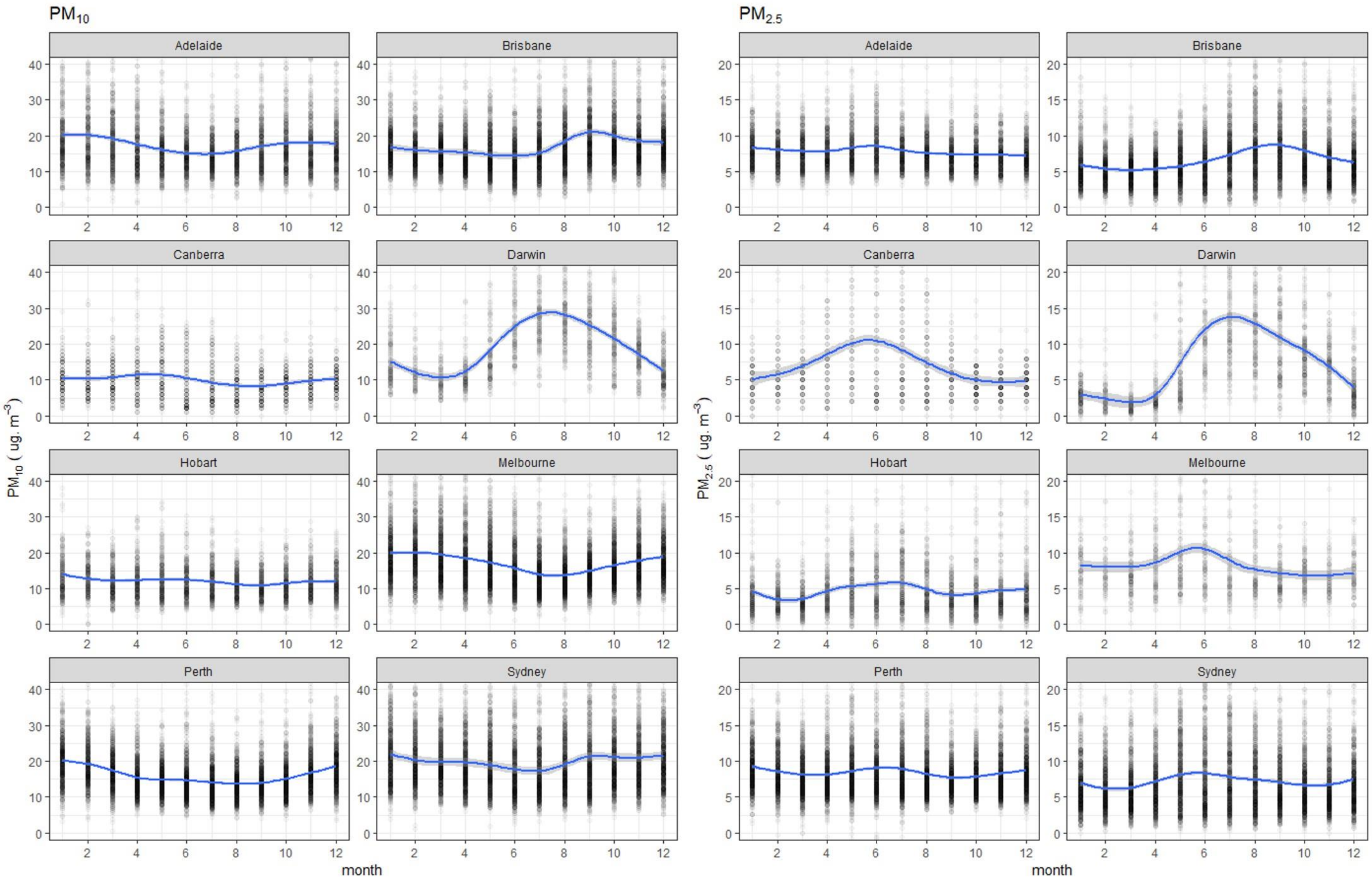

Figure 4. Seasonal trends of PM$_{10}$ and PM$_{2.5}$ per city using the generalised additive model (GAM).

3.4.3 Long-term trends

In the long-term trends obtained by GAM, some similarities can be observed such as the high particle mass concentrations from 2000 to 2005 then varying trends onwards (Figure 5) but there is no clear upward nor downward movement in the concentration trends for either metric. The highest PM_{10} concentrations were observed in Sydney in 2003, while the highest $PM_{2.5}$ concentrations occurred in Perth in 1997. Observations for the long-term trends in the different cities varied. There was a significant decline in PM_{10} in Adelaide in 2010 – 2011 but the decline was not apparent for $PM_{2.5}$. Then an opposite trend occurred in 2015 – 2016 with a substantial increase in $PM_{2.5}$ but not in PM_{10}. The concentration trends for Brisbane's PM_{10} and $PM_{2.5}$ were similar from 2000 onwards, but were opposite in earlier years. Comparing Brisbane and Sydney, a similar pattern was evident prior to Brisbane's peak PM concentration in 2010, but in Sydney, the PM_{10} was at a much higher range, and the $PM_{2.5}$ increased significantly in 2015.

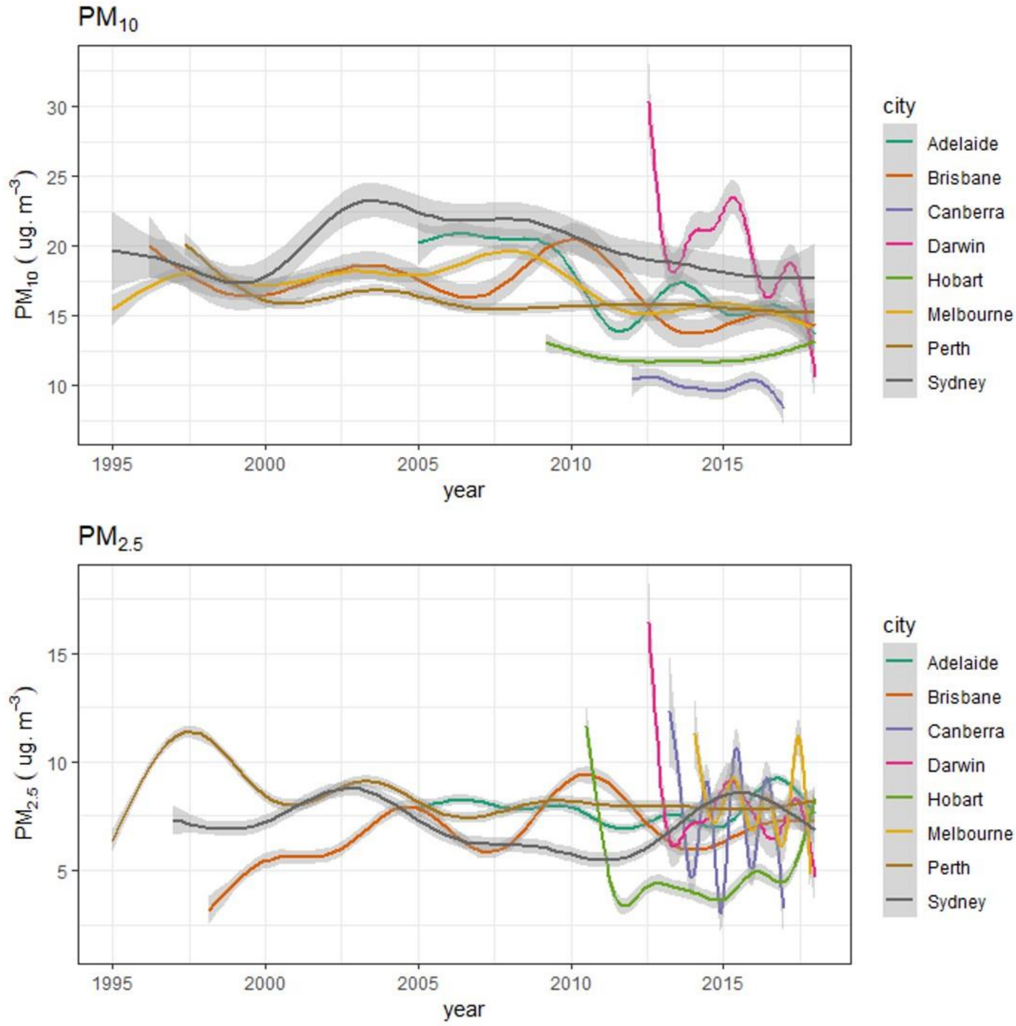

Figure 5. The long-term concentration trends per city using the generalised additive model (GAM).

Further, the PM_{10} in Canberra remained low over time and was the lowest among the capital cities, while its $PM_{2.5}$ was comparable to that of the other cities. The $PM_{2.5}$ trends in Melbourne and Hobart were comparable with Canberra being the most variable and Hobart the least variable. $PM_{2.5}$ concentrations showed higher variability within each year and from year to year than PM_{10} concentrations. Darwin's PM_{10} and $PM_{2.5}$ had similar pattern and both showed considerable variability in just 5 years. Perth's PM_{10} and $PM_{2.5}$ also followed the same pattern as that of Darwin, but Perth's PM concentrations were more constant.

3.5 Natural Factors affecting variability

PM levels are greatly affected by the prevailing winds (due to long-range transport and for dispersion) and the amount of precipitation (for wet deposition) (Barmpadimos et al., 2012; Pikridas et al., 2018; Querol et al., 2009). Therefore, variability in PM concentrations among the cities can also be attributed to differences in climate (i.e. the long-term weather pattern based on average temperature and precipitation of an area) and climate variability (i.e. brought about by climate phenomena such as El Niño Southern Oscillations). The climate systems of the capital cities have been presented in the introduction. For cities with the same climate type, the temperature and precipitation pattern coincide. Because most capital cities are located along the coastline, they receive more rainfall than central Australia. In general, the east coast, including the northern portion, is wetter than the west coast and the southern portion (BOM, 2010). Therefore, Adelaide and Perth receive less precipitation than the other capital cities, and experience less wet deposition.

Further, the prevailing wind direction and speed are comparable in cities with the same climate type, since wind is a derivative of temperature. In general, northern Australia is dominated by easterly winds, while the southern part is dominated by westerly winds. The wind pattern in Australian cities, as in all other places, is characterised by mornings with less wind than the afternoons, which are accompanied by inversions. Based on climate classification, Cfb type cities receive the most wind and Csa type cities receive the least wind (BOM, 2019). However, variability among cities with the same climate type has been observed; Adelaide and Sydney, which are colder compared to Perth and Brisbane, respectively, receive more wind especially in the afternoon. Additionally, land features and cityscape greatly affect the flow (Wang et al., 2018).

The differences in climate types and land features among the capital cities can also intensify the contribution of particular sources. For example, biomass burning (i.e. wildfires in the nearby savannah, prescribed burning to manage wildfires and burning of other vegetation for land clearing, for urban development or agricultural preparation) is a significant source in Darwin, especially during the warm and dry season (Hanigan et al., 2008), thus contributing to the high PM from May to November. Moreover, the fire scar (i.e. the blackened or charred land surface visible from satellites after bushfires) data from the North Australia and Rangelands Fire Information showed that an area with a radius of 25 km burns every year during the dry season in Darwin. The chance of dust storms also increases during the warm and dry seasons, with the south and southeast regions being the most vulnerable (Adelaide, Canberra, Melbourne, and Sydney). Wood heaters in Sydney contribute significantly to PM levels in winter, unlike in Brisbane, which is warmer throughout most of the year.

The effect of different climate types and seasonality can be further influenced by climate variability. The El Niño Southern Oscillation (ENSO) is a climate phenomenon related to changes in the Pacific Ocean, and is associated with either decreased rainfall (El Niño) or increased rainfall (La Niña) in northern and eastern Australia. The effects of El Niño are mostly felt over inland eastern Australia with varying impacts on southwest Western Australia and coastal NSW, while La Niña mostly influences northern and central Australia. For example, the high levels of PM in the early 2000s can be attributed to the extreme drought, particularly in southeastern Australia. The year 2009 was also a significantly dry year with many bushfires. In contrast, the declining PM_{10} concentrations observed in 2010 – 2011 may have been due to a La Niña event. The impacts of the ENSO have been correlated with PM_{10} variations in the Korean peninsula (Wie & Moon, 2017).

Another phenomenon affecting Australia is the Indian Ocean Dipole (IOD). A positive IOD tends to result in warmer days and below average spring rainfall in southern and central Australia, with a more severe fire season in the southeast, according to BOM. The Australian winter rainfall can also be reduced by a positive IOD, especially in the western and southern region extending to the southeast (Ashok et al., 2003). Moreover, when a neutral ENSO is forecast but a positive IOD exists, the influence of the IOD is more likely to dominate. In a study published by Cai et al. (2009), the bushfires in Victoria in February 2009 were linked to the occurrence of a positive IOD during that time rather than the effect of the El Niño.

3.6 Relationship of PM_{10} and $PM_{2.5}$ among cities

The PM_{10} and $PM_{2.5}$ concentrations among the cities showed varying correlations (Figure 6). The Pearson's *r*, confidence intervals and *p* values are given in Table S2. The mass concentrations of both Darwin and Perth had very weak to weak correlations with the mass concentrations of other capital cities (r = 0.01 – 0.15, p<0.05 for Darwin with Brisbane, Melbourne, Perth & Sydney and Perth with Adelaide, Brisbane, Darwin, Melbourne and Sydney for PM_{10} then Darwin with Canberra, Hobart & Melbourne and Perth with Canberra, Hobart & Melbourne for $PM_{2.5}$). Both the PM_{10} and $PM_{2.5}$ of Sydney and Brisbane were moderately correlated (r = 0.35 for PM_{10} and r = 0.16 for $PM_{2.5}$, p<0.05), similar to Canberra, Hobart and Melbourne (0.15 < r < 0.34 for PM_{10} and 0.17 < r < 0.29 for $PM_{2.5}$, p<0.05). Adelaide was moderately correlated with Melbourne only (r = 0.49 for PM_{10} and r = 0.31 for $PM_{2.5}$, p<0.05) while Canberra was also moderately correlated with Sydney (r = 0.51 for both PM_{10} and $PM_{2.5}$, p<0.05). These weak correlations among cities can also be observed from the varying concentration trends obtained by GAM (Figure 5).

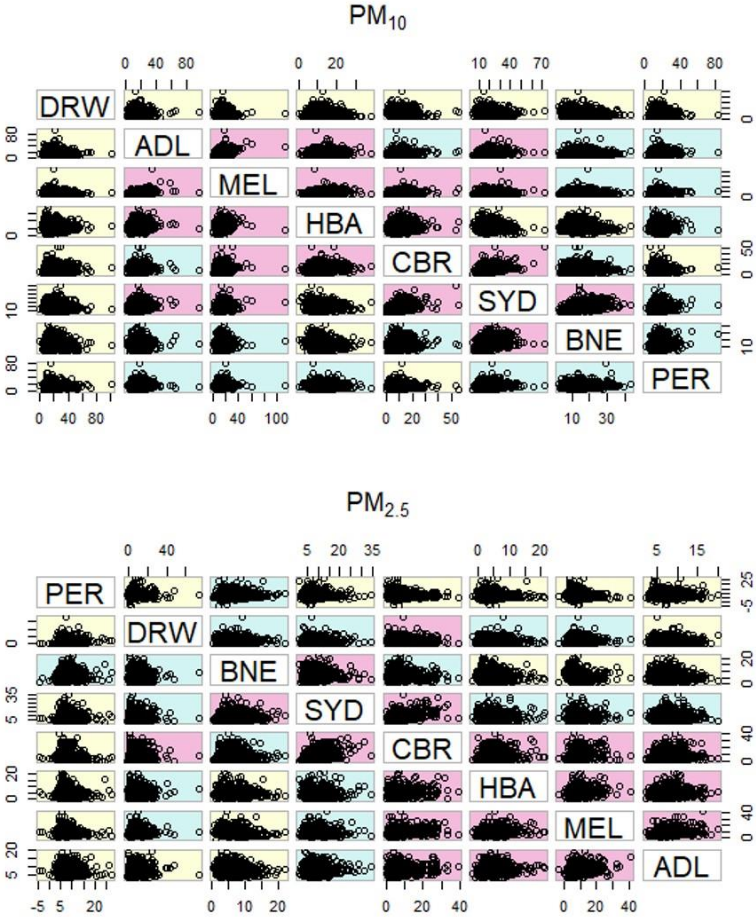

Figure 6. Correlation among the cities (pink = moderate correlation, blue = weak correlation, yellow = very weak correlation).

Finally, the cities were clustered based on data similarities and patterns. There were six principal components identified by principal component analysis based on eigenvalues and the cumulative proportion of the variance, which covers 94.9% and 93.6% for PM_{10} and $PM_{2.5}$, respectively. The membership degrees matrix produced by fuzzy c-means is shown in Table S3. The results of clustering coincided with the PM_{10} and $PM_{2.5}$ median plot (Figure 7). Canberra and Hobart both had low PM_{10} and $PM_{2.5}$. Brisbane, Darwin, and Sydney had similar $PM_{2.5}$ concentrations but varying PM_{10} concentrations. Adelaide, Melbourne, and Perth had similar PM_{10} concentrations but slightly varying $PM_{2.5}$ concentrations.

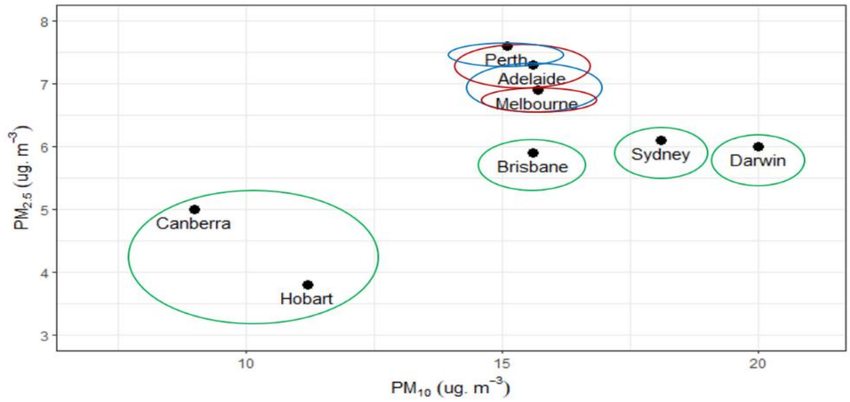

Figure 7. Median of the daily PM_{10} and $PM_{2.5}$ and clustering of cities using fuzzy c-means (blue = clustering for PM_{10}, red = clustering for $PM_{2.5}$, green = clustering for both PM_{10} and $PM_{2.5}$).

Canberra and Hobart have the same climate classification (Cfb) (although, Canberra's summer is hotter while it is colder for the rest of the year compared to Hobart) and both have low population and low vehicle numbers, which may explain why they are clustered together. The higher PM_{10} in Hobart may be attributed to the contribution of sea salts and aged particles from mainland Australia. Melbourne has the same climate type as Canberra and Hobart, but has more emission sources particularly from vehicles, resulting in higher particulate mass concentrations and a separate cluster. Similar conditions can be observed with Brisbane and Sydney, and also Perth and Adelaide, which have the same climate category but different magnitudes of emissions. Additionally, the higher PM_{10} in Adelaide and in Sydney compared with Perth and Brisbane, may be due to the contribution of stronger winds in Adelaide and Sydney causing more resuspension, and the higher precipitation rate in Perth and Brisbane causing a "washing" effect. The high PM_{10} in Adelaide and Melbourne compared with the cities of the same climate type may be due to the contributions of dust storms. Lastly, Darwin, being the only tropical city, has its own cluster. The clustering results are also reflected in the correlations between cities; Darwin's PM concentrations are only weakly correlated with other cities.

4. Conclusion

The PM concentrations in Australian capital cities are relatively low and daily concentrations are within the country's daily standards at least 95% of the time. Mean concentrations are within the annual standards as well as the WHO guideline values. Despite increased motor vehicle activity, vigorous economic growth and an expanding population, the daily concentrations of both PM_{10} and $PM_{2.5}$ have decreased over the years, though the rate is small. The decrease in PM_{10} may be the result of Australia's changing geochemical and sedimentary systems due to agricultural and industrial development (Marx et al., 2014). For $PM_{2.5}$, the effectiveness of emission controls may not be as obvious as those in the case of Beijing caused by the impacts of meteorology as illustrated Vu et al. (2019).

Both long-term and seasonal trend variability among the cities can be attributed to differences in meteorological conditions and the impacts of particular sources at certain seasons (e.g. wood heaters in winter and bushfires in summer). Therefore, strategies to control inevitable emissions such as the techniques suggested by Hart and Jiang (2018) and F. H. Johnston et al. (2013) to improve emissions from burns and wood heaters, respectively, also have a role to play. Regulations for reducing emissions from traffic (e.g. improved fuel and vehicle technology) and energy production (e.g. increased use of renewable sources) are still significant to counter the effect of increasing population, increasing demand for energy and climate change (i.e. increasing temperature, decreasing amount of precipitation and more severe impacts of ENSO and IOD causing bushfires and dust storms). Consequently, the PM concentration in Australia's capital cities may already be at its regional background level, from which further improvement can be challenging.

Acknowledgement

The authors would like to acknowledge the following for their valuable support for this research and for providing the data of their respective cities.

Ningbo Jiang – Department of Planning, Industry & Environment NSW

John Innis – EPA Tasmania

Arthur Grieco – Department of Water and Environmental Regulation WA

Swarup Chatterrjee and Ian Fox – ACT Health

Don Neale – Department of Environment and Science QLD

Melinda Hunt and Andrew Partidge– Environmental Protection Authority SA

References

Aryal, R., Beecham, S., Kamruzzaman, M., Conner, S., & Lee, B.-K. (2015). Temporal change of PM 10 and its mass fraction during a dust storm in September 2009 in Australia. *Air Qual. Atmos. Hlth., 8*(5), 483-494. doi:10.1007/s11869-014-0297-0

Ashok, K., Guan, Z., & Yamagata, T. (2003). Influence of the Indian Ocean Dipole on the Australian winter rainfall. *Geophys. Res. Lett., 30*(15), n/a-n/a. doi:10.1029/2003GL017926

Barmpadimos, I., Keller, J., Oderbolz, D., Hueglin, C., & Prévôt, A. S. H. (2012). One decade of parallel fine (PM2.5) and coarse (PM10–PM2.5) particulate matter measurements in Europe: trends and variability. *Atmos. Chem. Phys., 12*(7), 3189-3203. doi:10.5194/acp-12-3189-2012

BOM. (2010). *Average annual, seasonal and monthly rainfall*. Commonwealth of Australia. Retrieved November 04, 2019 from http://www.bom.gov.au/jsp/ncc/climate_averages/rainfall/index.jsp

BOM. (2019). *Wind Roses for Selected Locations in Australia*. Commonwealth of Australia. Retrieved November 03, 2019 from http://www.bom.gov.au/climate/averages/wind/selection_map.shtml

Broome, R. A., Cope, M. E., Goldsworthy, B., Goldsworthy, L., Emmerson, K., Jegasothy, E., & Morgan, G. G. (2016). The mortality effect of ship-related fine particulate matter in the Sydney greater metropolitan region of NSW, Australia. *Environ. Int., 87*, 85-93. doi:10.1016/j.envint.2015.11.012

Cai, W., Cowan, T., & Raupach, M. (2009). Positive Indian Ocean Dipole events precondition southeast Australia bushfires. *Geophys. Res. Lett., 36*(19), n/a-n/a. doi:10.1029/2009GL039902

Cebeci, Z., Yildiz, F., Kavlak, A. T., Cebeci, C., & Onder, H. (2019). Probabbilistic and Possibilistic Cluster Analysis.

CSIRO. (2001). *A Pilot Study of Air Quality in Darwin, N.T.* . Commonwealth Scientific and Industrial Research Organisation. Retrieved January 24, 2020 from https://ntepa.nt.gov.au/__data/assets/pdf_file/0006/284982/aqstudy.pdf

DNRME. (2019). *Electricity Generation Map*. Queensland: Queensland Government. Retrieved November 1, 2019 from https://maps.dnrm.qld.gov.au/electricity-generation-map/

Dogruparmak, S. C., Keskin, G. A., Yaman, S., & Alkan, A. (2014). Using principal component analysis and fuzzy c–means clustering for the assessment of air quality monitoring. *Atmos. Pollut. Res., 5*(4), 656-663. doi:10.5094/APR.2014.075

Emmerson, K. M., Galbally, I. E., Guenther, A. B., Paton-Walsh, C., Guerette, E. A., Cope, M. E., Keywood, M. D., Lawson, S. J., Molloy, S. B., Dunne, E., Thatcher, M., Karl, T., & Maleknia, S. D. (2016). Current estimates of biogenic emissions from eucalypts uncertain for southeast Australia. *Atmos. Chem. Phys., 16*(11), 6997-7011. doi:10.5194/acp-16-6997-2016

Friend, A. J., & Ayoko, G. A. (2009). Multi-criteria ranking and source apportionment of fine particulate matter in Brisbane, Australia. *Environ. Chem., 6*(5), 398-406. doi:10.1071/EN09035

Hanigan, I. C., Johnston, F. H., & Morgan, G. G. (2008). Vegetation fire smoke, indigenous status and cardio-respiratory hospital admissions in Darwin, Australia, 1996–2005: a time-series study. *Environ. Health, 7*(1), 42-42. doi:10.1186/1476-069X-7-42

Hart, M., & Jiang, N. (2018). Meteorological controls on atmospheric particulate pollution during hazard reduction burns. *Atmos. Chem. Phys., 18*(9), 6585-6599. doi:10.5194/acp-18-6585-2018

He, C., Miljevic, B., Crilley, L. R., Surawski, N. C., Bartsch, J., Salimi, F., Uhde, E., Schnelle-Kreis, J., Orasche, J., Ristovski, Z., Ayoko, G. A., Zimmermann, R., & Morawska, L.

(2016). Characterisation of the impact of open biomass burning on urban air quality in Brisbane, Australia. *Environ. Int., 91*, 230-242. doi:10.1016/j.envint.2016.02.030
Hurley, C. (2019). Clustering Graphics. Retrieved from https://CRAN.R-project.org/package=gclus
Hutchinson, M. F., McIntyre, S., Hobbs, R. J., Stein, J. L., Garnett, S., & Kinloch, J. (2005). Integrating a global agro-climatic classification with bioregional boundaries in Australia. *Global Ecol. Biogeogr., 14*(3), 197-212. doi:10.1111/j.1466-822X.2005.00154.x
Hyndman, R., Athanasopoulos, G., Bergmeir, C., Caceres, G., Chhay, L., O'Hara-Wild, M., Petropoulos, F., Razbash, S., Wang, E., & Yasmeen, F. (2018). Forecasting functions for time series and linear models. Retrieved from http://pkg.robjhyndman.com/forecast
Innis, J., Bell, A., Smeal, A., Groth, M., Kuchinke, C., & Hyde, B. (2013). *Comparing Tasmanian PM10 and PM2.5 TEOM AND Low Volume Air Sampler Data*. Paper presented at the Clean Air Society of Aus/NZ, Sydney. https://epa.tas.gov.au/Pages/Document.aspx?docid=2289
Johnston, F. H., Hanigan, I. C., Henderson, S. B., & Morgan, G. G. (2013). Evaluation of interventions to reduce air pollution from biomass smoke on mortality in Launceston, Australia: retrospective analysis of daily mortality, 1994-2007. *BMJ-Brit. Med J., 346*(7890). doi:10.1136/bmj.e8446
Johnston, F. H., Hanigan, I. C., Henderson, S. B., Morgan, G. G., Portner, T., Williamson, G. J., & Bowman, D. M. J. S. (2011). Creating an Integrated Historical Record of Extreme Particulate Air Pollution Events in Australian Cities from 1994 to 2007. *J. Air Waste Manage. Assoc., 61*(4), 390-398. doi:10.3155/1047-3289.61.4.390
Johnston, O., Johnston, F., Todd, J., & Williamson, G. (2016). Community-Wide Distribution of a Catalytic Device to Reduce Winter Ambient Fine Particulate Matter from Residential Wood Combustion: A Field Study. *PloS one, 11*(11), e0166677-e0166677. doi:10.1371/journal.pone.0166677
Jordan, T. B., Seen, A. J., Jacobsen, G. E., & Gras, J. L. (2006). Radiocarbon determination of woodsmoke contribution to air particulate matter in Launceston, Tasmania. *Atmos. Environ., 40*(14), 2575-2582. doi:10.1016/j.atmosenv.2005.12.024
Junkermann, W., & Hacker, J. (2015). Ultrafine particles over Eastern Australia: an airborne survey. *Tellus B Chem. Phys. Meteorol., 67*(1). doi:10.3402/tellusb.v67.25308
Keywood, M. D., Emmerson, K. M., & Hibberd, M. F. (2016). *Ambient air quality: Pressures. In: Australia state of the environment 2016*. Canberra: Australian Government Department of the Environment and Energy. Retrieved March 02, 2020 from https://soe.environment.gov.au/theme/ambient-air-quality/framework/pressures
Li, C., Martin, R. V., van Donkelaar, A., Boys, B. L., Hammer, M. S., Xu, J.-W., Marais, E. A., Reff, A., Strum, M., Ridley, D. A., Crippa, M., Brauer, M., & Zhang, Q. (2017). Trends in Chemical Composition of Global and Regional Population-Weighted Fine Particulate Matter Estimated for 25 Years. *Environ. Sci. Technol., 51*(19), 11185-11195. doi:10.1021/acs.est.7b02530
Marx, S. K., McGowan, H. A., Kamber, B. S., Knight, J. M., Denholm, J., & Zawadzki, A. (2014). Unprecedented wind erosion and perturbation of surface geochemistry marks the Anthropocene in Australia. *J. Geophys. Res. Earth Surf., 119*(1), 45-61. doi:10.1002/2013JF002948
Masiol, M., Squizzato, S., Chalupa, D. C., Utell, M. J., Rich, D. Q., & Hopke, P. K. (2018). Long-term trends in submicron particle concentrations in a metropolitan area of the northeastern United States. *Sci. Total Environ., 633*, 59-70. doi:10.1016/j.scitotenv.2018.03.151
Massoud, R., Shihadeh, A. L., Roumié, M., Youness, M., Gerard, J., Saliba, N., Zaarour, R., Abboud, M., Farah, W., & Saliba, N. A. (2011). Intraurban variability of PM10 and PM2.5 in an Eastern Mediterranean city. *Atmos. Res., 101*(4), 893-901. doi:10.1016/j.atmosres.2011.05.019

Mazaheri, M., Johnson, G. R., & Morawska, L. (2011). An inventory of particle and gaseous emissions from large aircraft thrust engine operations at an airport. *Atmos. Environ., 45*(20), 3500-3507. doi:10.1016/j.atmosenv.2010.12.012

McTainsh, G. H., Lynch, A. W., & Tews, E. K. (1998). Climatic controls upon dust storm occurrence in eastern Australia. *J. Arid Environ., 39*(3), 457-466. doi:10.1006/jare.1997.0373

Mészaros, D., Markos, J., Fitzgerald, D. G., Walters, E. H., & Wood-Baker, R. (2015). An observational study of PM10 and hospital admissions for acute exacerbations of chronic respiratory disease in Tasmania, Australia 1992-2002. *BMJ Open Respir. Res., 2*(1). doi:10.1136/bmjresp-2014-000063

Mohsen, M., Ahmed, M. B., & Zhou, J. L. (2018). Particulate matter concentrations and heavy metal contamination levels in the railway transport system of Sydney, Australia. *Transport. Res. D-TR E, 62*, 112-124. doi:10.1016/j.trd.2018.02.015

Pandolfi, M., Alastuey, A., Pérez, N., Reche, C., Castro, I., Shatalov, V., & Querol, X. (2016). Trends analysis of PM source contributions and chemical tracers in NE Spain during 2004-2014: a multi-exponential approach. *Atmos. Chem. Phys., 16*(18), 11787-11805. doi:10.5194/acp-16-11787-2016

Pikridas, M., Vrekoussis, M., Sciare, J., Kleanthous, S., Vasiliadou, E., Kizas, C., Savvides, C., & Mihalopoulos, N. (2018). Spatial and temporal (short and long-term) variability of submicron, fine and sub-10 μm particulate matter (PM1, PM2.5, PM10) in Cyprus. *Atmos. Environ., 191*, 79-93. doi:10.1016/j.atmosenv.2018.07.048

Pohlert, T. (2018). Non-Parametric Trend Tests and Change-Point Detection. Retrieved from https://CRAN.R-project.org/package=trend

Qadir, R. M., Schnelle-Kreis, J., Abbaszade, G., Arteaga-Salas, J. M., Diemer, J., & Zimmermann, R. (2014). Spatial and temporal variability of source contributions to ambient PM10 during winter in Augsburg, Germany using organic and inorganic tracers. *Chemosphere, 103*, 263-273. doi:10.1016/j.chemosphere.2013.12.015

Querol, X., Alastuey, A., Pey, J., Cusack, M., Pérez, N., Mihalopoulos, N., Theodosi, C., Gerasopoulos, E., Kubilay, N., & Koçak, M. (2009). Variability in regional background aerosols within the Mediterranean. *Atmos. Chem. Phys., 9*(14), 4575-4591. doi:10.5194/acp-9-4575-2009

R Core Team. (2018). The R Stats Package.

Rea, G., Paton-Walsh, C., Turquety, S., Cope, M., & Griffith, D. (2016). Impact of the New South Wales fires during October 2013 on regional air quality in eastern Australia. *Atmos. Environ., 131*(C), 150-163. doi:10.1016/j.atmosenv.2016.01.034

Revelle, W. (2019). Procedures for Psychological, Psychometric, and Personality Research. Retrieved from https://personality-project.org/r/psych

RStudio Team. (2016). RStudio: Integrated Development for R. RStudio, Inc. Boston, MA. Retrieved from http://www.rstudio.com

Shahsavani, A., Naddafi, K., Jafarzade Haghighifard, N., Mesdaghinia, A., Yunesian, M., Nabizadeh, R., Arahami, M., Sowlat, M. H., Yarahmadi, M., Saki, H., Alimohamadi, M., Nazmara, S., Motevalian, S. A., & Goudarzi, G. (2012). The evaluation of PM10, PM2.5, and PM1 concentrations during the Middle Eastern Dust (MED) events in Ahvaz, Iran, from april through september 2010. *J. Arid Environ., 77*, 72-83. doi:10.1016/j.jaridenv.2011.09.007

Sharma, A. P., Kim, K. H., Ahn, J. w., Shon, Z. H., Sohn, J. R., Lee, J. H., Ma, C. J., & Brown, R. J. C. (2014). Ambient particulate matter (PM10) concentrations in major urban areas of Korea during 1996–2010. *Atmos. Pollut. Res., 5*(1), 161-169. doi:10.5094/APR.2014.020

Sugimoto, N., Shimizu, A., Matsui, I., & Nishikawa, M. (2016). A method for estimating the fraction of mineral dust in particulate matter using PM2.5-to-PM10 ratios. *Particuology, 28*, 114-120. doi:10.1016/j.partic.2015.09.005

Tadros, C. V., Crawford, J., Treble, P. C., Baker, A., Cohen, D. D., Atanacio, A. J., Hankin, S., & Roach, R. (2018). Chemical characterisation and source identification of

atmospheric aerosols in the Snowy Mountains, south-eastern Australia. *Sci. Total Environ., 630*, 432-443. doi:10.1016/j.scitotenv.2018.02.231
Taylor, M. P., & Isley, C. F. (2014). Measuring, monitoring and reporting but not intervening: Air quality in Australian mining and smelting areas. *Air Qual. Clim. Change, 48*(2), 35-42.
The Lancet. (2020). Australia on fire. *The Lancet, 395*(10219), 165. doi:10.1016/S0140-6736(20)30098-2
Vu, T. V., Shi, Z., Cheng, J., Zhang, Q., He, K., Wang, S., & Harrison, R. M. (2019). Assessing the impact of clean air action on air quality trends in Beijing using a machine learning technique. *Atmos. Chem. Phys., 19*(17), 11303-11314. doi:10.5194/acp-19-11303-2019
Wang, X., Dickinson, R. E., Su, L., Zhou, C., & Wang, K. (2018). PM2.5 Pollution in China and How It Has Been Exacerbated by Terrain and Meteorological Conditions. *Bull. Amer. Meteor. Soc., 99*(1), 105-119. doi:10.1175/bams-d-16-0301.1
Wickham, H. (2009). *ggplot2: Elegant Graphics for Data Analysis*: Springer-Verlag New York.
Wie, J., & Moon, B.-K. (2017). ENSO-related PM10 variability on the Korean Peninsula. *Atmos. Environ., 167*, 426-433. doi:10.1016/j.atmosenv.2017.08.052
WPR. (2019). Developed Countries List Population. Retrieved from http://worldpopulationreview.com/countries/developed-countries/
Yadav, V., & Turner, J. (2014). Gauging intraurban variability of ambient particulate matter arsenic and other air toxic metals from a network of monitoring sites. *Atmos. Environ., 89*, 318-328. doi:10.1016/j.atmosenv.2014.02.030
Zhao, D., Chen, H., Yu, E., & Luo, T. (2019). PM2.5/PM10 Ratios in Eight Economic Regions and Their Relationship with Meteorology in China. *Adv. Meteorol., 2019*, 15. doi:10.1155/2019/5295726

Two decades of trends in urban particulate matter concentrations across Australia

Supplementary Material

Table S1. Monitoring Stations in all capital cities understudy.

City/Stations	Siting and Sources
Adelaide, South Australia	
Adelaide CBD	Located adjacent to Victoria Square, the centre of the CBD.
Le Fevre 2	Located in Le Fevre Peninsula, the station is 18 km NW of the CBD, which has a mix of industry and residential land uses.
Netley	Western industrial suburban area, adjacent to Adelaide airport, with the station sited 5 km W of CBD and beside the Transport Avenue, which always has heavy traffic.
Brisbane, Queensland	
Rocklea	The area is residential with light industry. The station located in Oxley Creek Common, 8 km SW of CBD with Sherwood road 160 m away.
South Brisbane	This commercial area is just 2 km SE of the CBD and the station is adjacent to the South East Freeway (30 m away)
Springwood	Residential area 20 km SE of CBD. The station is located in a school and 1 km away from the South East Freeway.
Woolloongabba	Station is within a commercial business area, located in a kerb of a busy main road (8 m away from Ipswich road), 3 km SSE of CBD.
Canberra, Australian Capital Territory	
Civic	The station is at the western side of the Olympic swimming pool, sited in a carpark and adjacent to Allara Street (6 m). This area is the city centre (CBD) of Canberra with mostly commercial buildings.
Florey	Sited on a public land at the end of Neumann Place with nearest road at 150 m. The area is a residential suburb, 10 km NW of the CBD.
Monash	Located in the Monash district playing fields approximately 300 m of the Cockcroft Avenue, in a residential area, 15 km SSW of the CBD.
Darwin, Northern Territory	
Palmerston	This station is located in light bushland approximately 4 km SW of Palmerston, 13 km ESE of CBD and provides information on airborne pollutants moving from the industrial activities in the Middle Harbor.
Winnellie	The station is sited in a residential/light industrial area between the northern suburbs and the CBD (7 km away NE), the two most densely populated areas in the Territory.
Hobart, Tasmania	
Hobart	The station is located in a residential area of New Town, 3.5 km away WNW of the CBD.
Launceston	This monitoring station is sited in the NE corner of a waste water treatment plant on the banks of the Tamar River in Ti Tree Bend. About 40 km NW of Launceston, a heavy Industrial area is located at Bell Bay
Melbourne, Victoria	
Alphington	The station is sited next to a railway station and Wingrove Street in a residential/light industrial area. Alphington suburb is located 7 km NE of the CBD.
Footscray	An inner-western suburb 6 km NW of the CBD. The area is residential/industrial and the station is sited inside the Hansen Reserve.
Perth, Western Australia	
Caversham	This metropolitan suburb is in the Swan Valley, a grape growing region located 14 km NE of the CBD and next to the Perth foothills. It has low density housing and paddocks with some brick manufacturing.
Duncraig	A northern suburb, 16 km NNW of the CBD, with moderate to high housing density and traffic flow. The site is 200 m W of the Mitchell Freeway, a main north-south arterial road carrying approximately 98,000 vehicles daily.
South Lake	This SE metropolitan site is 17 km S of the CBD and with moderate to high housing density and traffic flow. It is located 1.6 km W of the Kwinana freeway carrying approximately 87,000 vehicles daily and 4 km NE of the Kwinana industrial area.
Sydney, New South Wales	
Chullora	The station is located at Southern Sydney TAFE in Worth Street, 15 km W of the CBD, to monitor the East Sydney region. The area is at the centre of the Sydney Basin with mixed residential and commercial land uses.
Earlwood	Also monitoring the East Sydney region, the station is located in Beaman Park in mostly residential area in the Cook's River Valley, about 9 km SW of the CBD.
Liverpool	This station is in a mixed residential and commercial area, sited in the Council depot, off Rose Street, 29 km W of the CBD, monitoring the South-west Sydney region.
Richmond	Located inside the University of Western Sydney, 51 km NW of the Sydney CBD, in the residential/semi-rural area of the Hawkesbury basin, monitoring the North-west Sydney Region.

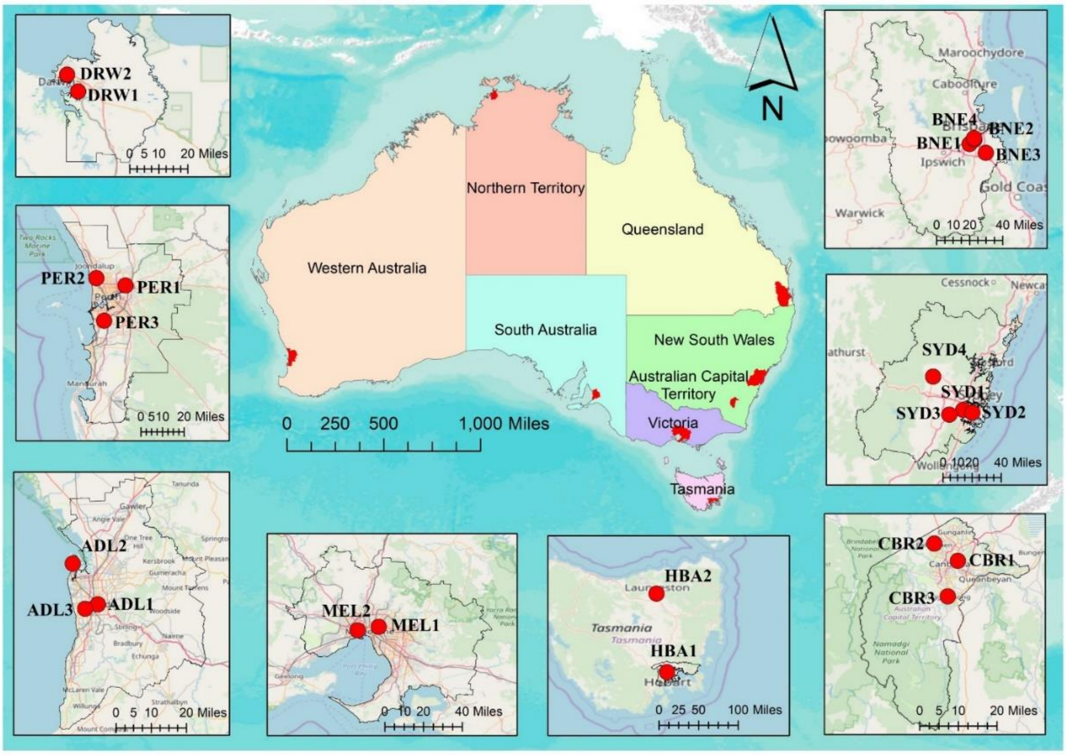

Figure S1. Location of the monitoring stations used in this study.

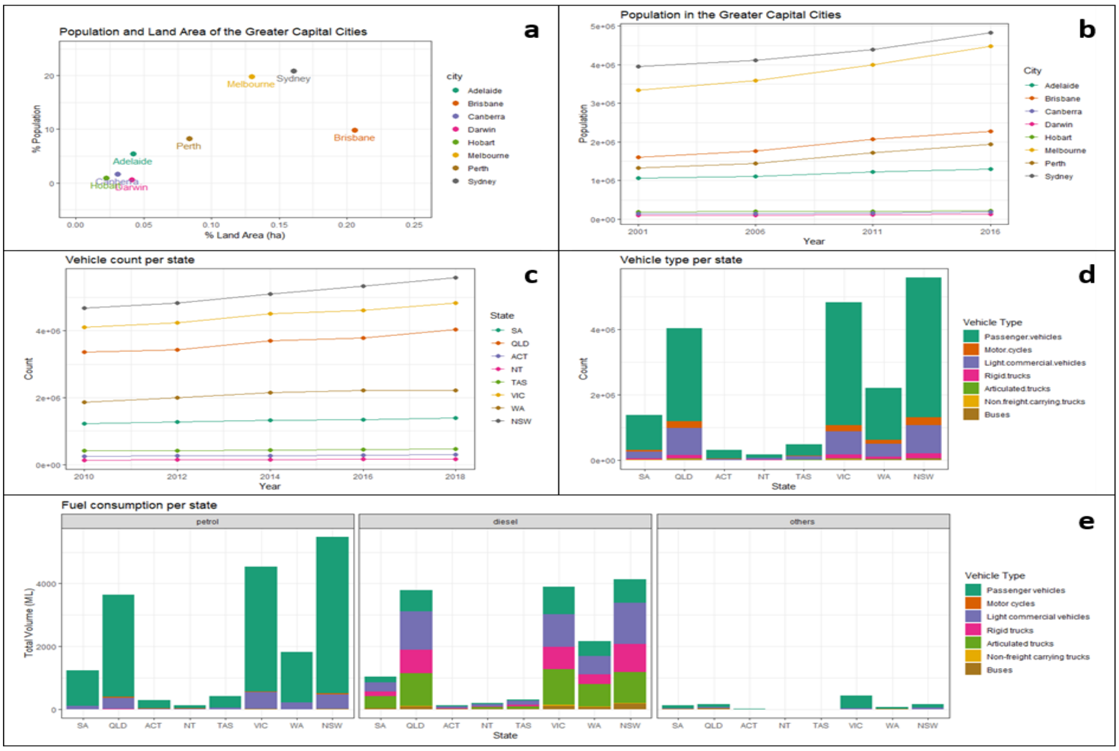

Note: Australian states: South Australia (SA), Queensland (QLD), Australian Capital Territory (ACT), Northern Territory (NT), Tasmania (TAS), Victoria (VIC), Western Australia (WA) and New South Wales (NSW).

Figure S2. (a) Percent population (2018) and percent land area of each greater capital city to Australia. (b) Population size and growth in the greater capital cities. (c) Total motor vehicle registration by state/territory. (d) Motor vehicle registration by type by state/territory from the period 1 July 2017 to 30 June 2018. (e) Total fuel consumption per vehicle type by state/territory from the period 1 July 2017 to 30 June 2018; fuel types under *others* include LPG/CNG/dual fuel/hybrid and others. Data Source: Australian Bureau of Statistics (2019).

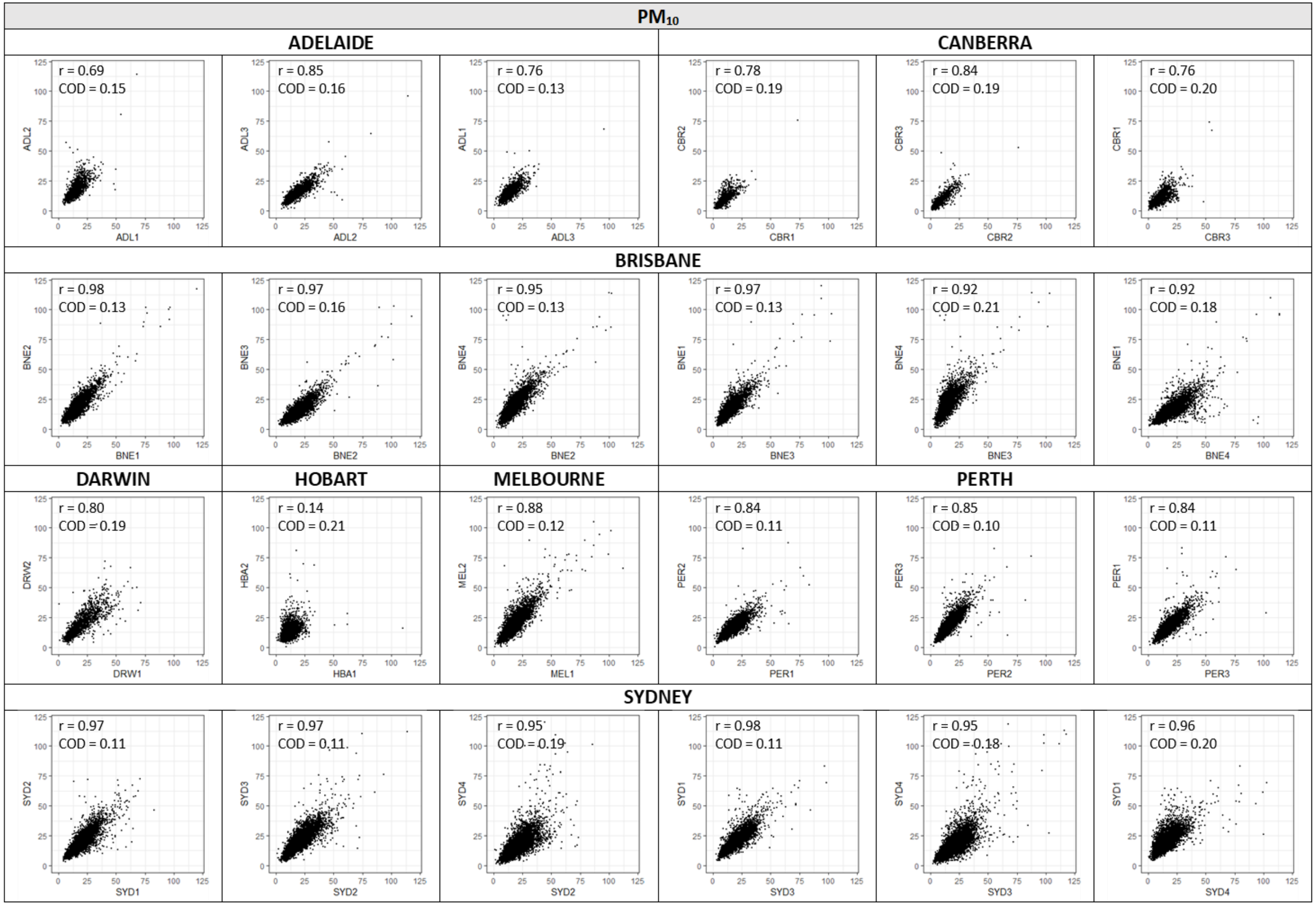

Figure S3. Pearson's correlation (*r*) with all p<0.001 and the coefficient of divergence (COD) for the daily PM_{10} concentrations for all monitoring stations in the Australian capital cities.

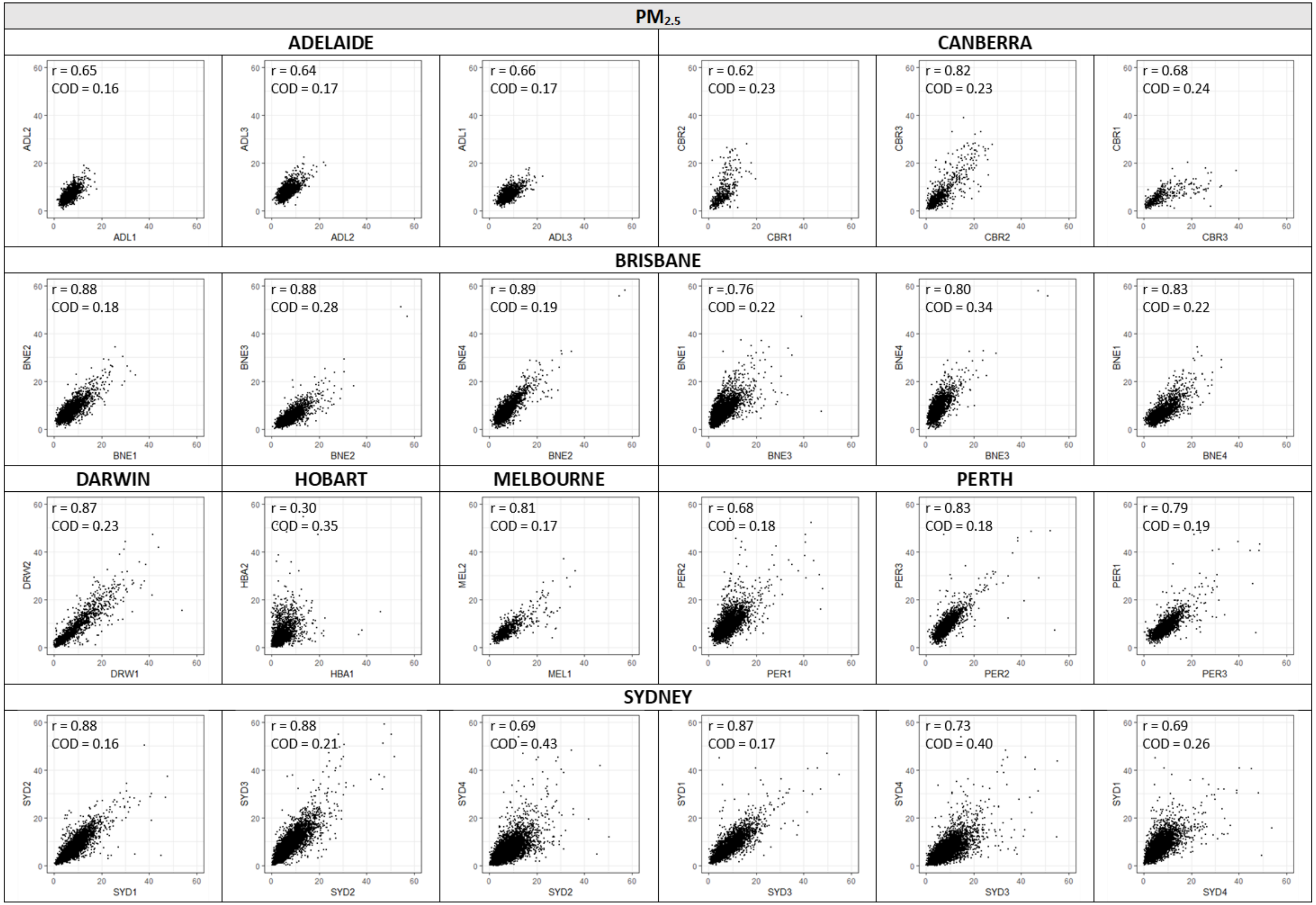

Figure S4. Pearson's correlation (*r*) with all $p<0.001$ and the coefficient of divergence (COD) for the daily $PM_{2.5}$ concentrations for all monitoring stations in the Australian capital cities.

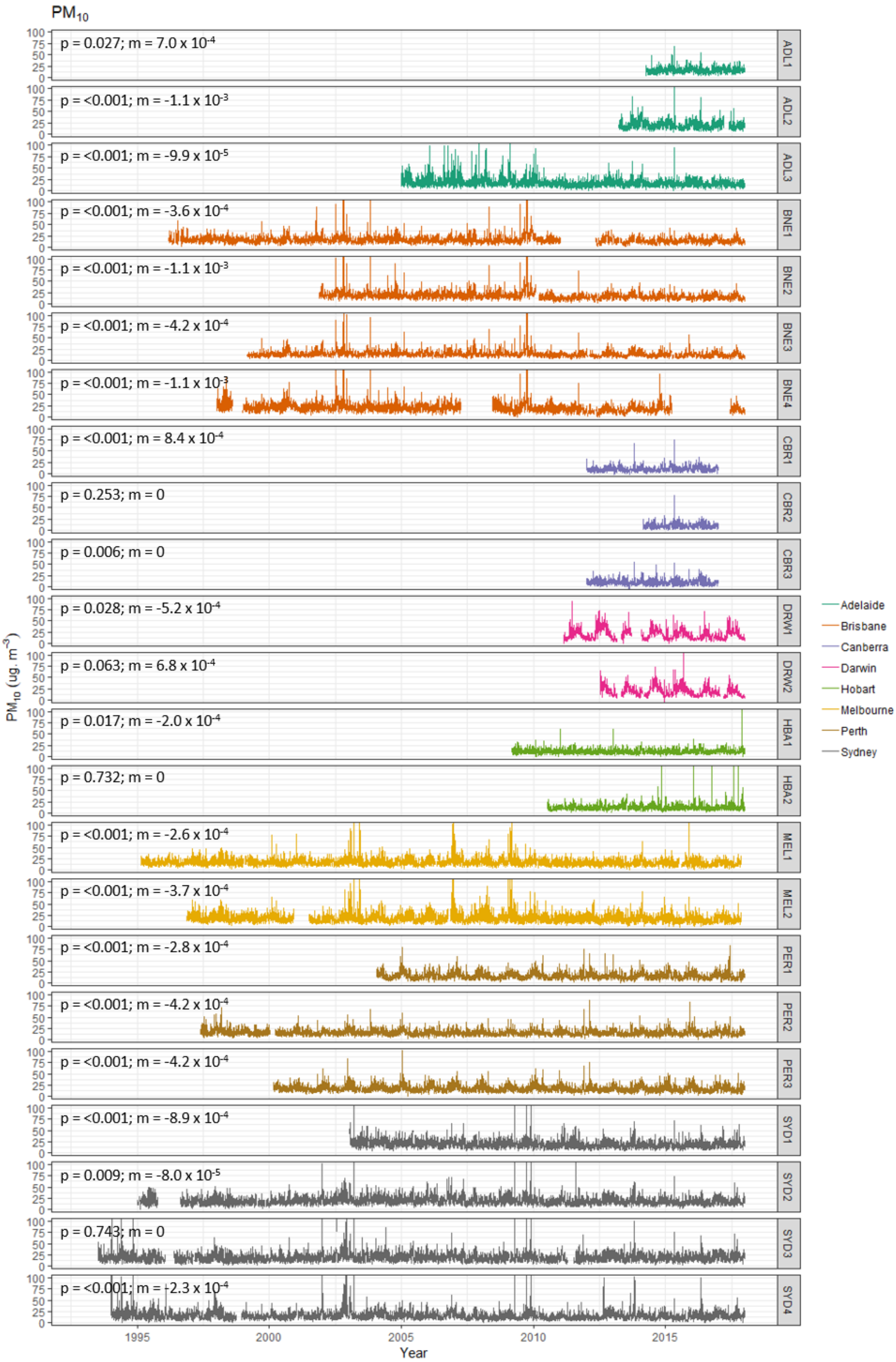

Figure S5. Time series plot of the daily PM_{10} concentrations for all monitoring stations in the Australian capital cities with the Mann-Kendall trend test result (a monotonic trend exist if *p*<0.05) and the Sen's slope (m in $\mu g.m^{-3}.yr^{-1}$).

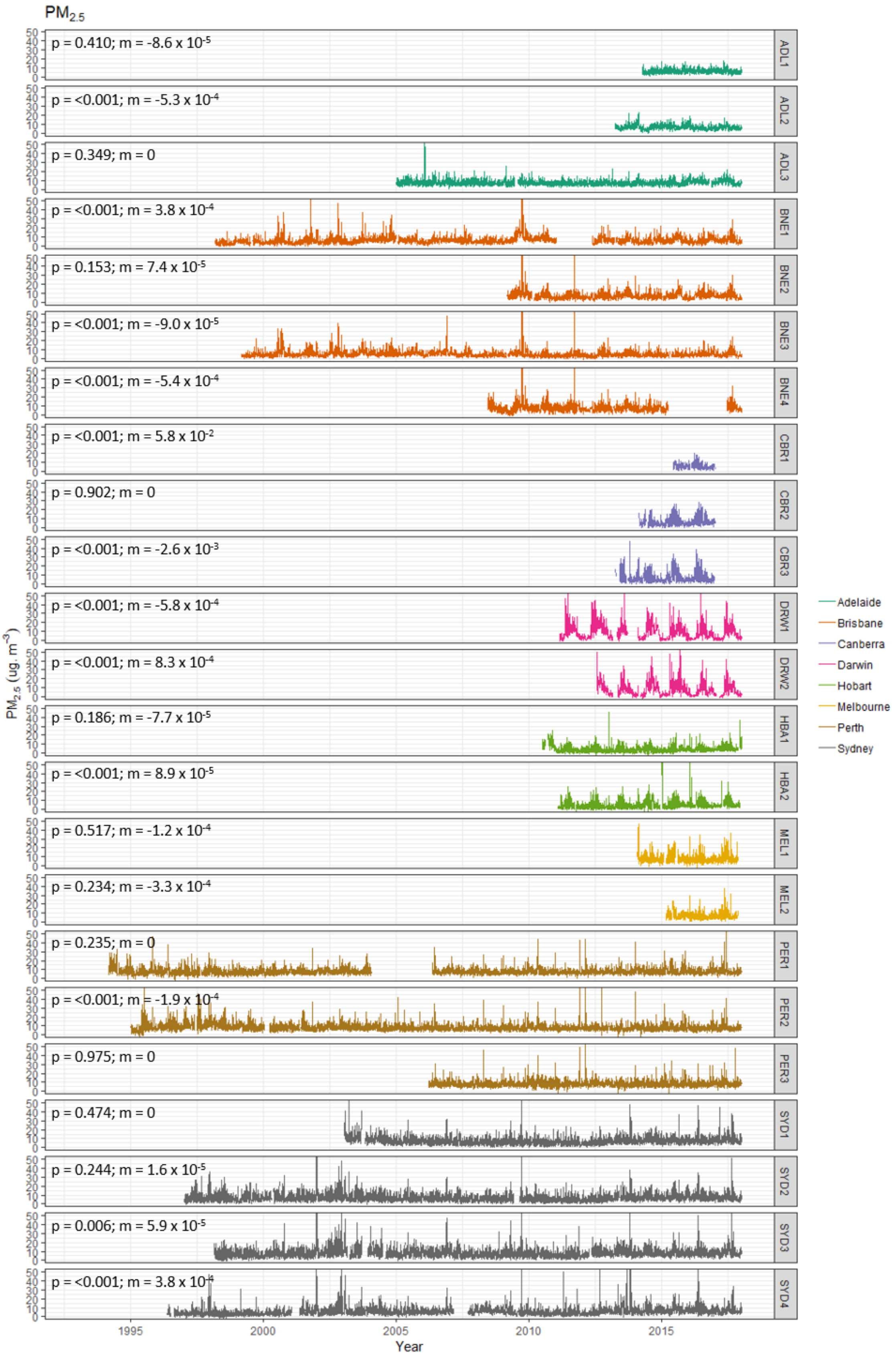

Figure S6. Time series plot of the daily $PM_{2.5}$ concentrations for all monitoring stations in the Australian capital cities with the Mann-Kendall trend test result (a monotonic trend exist if $p<0.05$) and the Sen's slope (m in $\mu g.m^{-3}.yr^{-1}$).

Table S2. Pearson's correlation coefficient (*r*) of the PM concentrations per city.

	ADL	BNE	CBR	DRW	HBA	MEL	PER	SYD
Adelaide	**1.000**	0.067* [0.013, 0.120]	0.121* [0.068, 0.173]	-0.043 [-0.096, 0.011]	0.207* [0.155, 0.258]	0.486* [0.444, 0.526]	0.120* [0.067, 0.172]	0.184* [0.131, 0.235]
Brisbane	-0.189* [-0.254, -0.123]	**1.000**	0.079* [0.025, 0.132]	-0.107* [-0.160, -0.054]	-0.128* [-0.180, -0.074]	0.007 [-0.047, 0.060]	0.146* [0.093, 0.198]	0.353* [0.306, 0.400]
Canberra	0.125* [0.057, 0.192]	0.007 [-0.061, 0.075]	**1.000**	-0.030 [-0.084, 0.023]	0.153* [0.100, 0.205]	0.219* [0.167, 0.270]	-0.016 [-0.069, 0.038]	0.511* [0.470, 0.550]
Darwin	-0.061 [-0.129, 0.007]	0.064 [-0.004, 0.132]	0.107* [0.039, 0.174]	**1.000**	-0.044 [-0.098, 0.009]	-0.113* [-0.166, -0.060]	-0.111* [-0164, -0.058]	-0.082* [-0.135, -0.029]
Hobart	0.095* [0.027, 0.162]	-0.080* [-0.147, -0.011]	0.171* [0.104, 0.237]	0.088* [0.202, 0.156]	**1.000**	0.344* [0.296, 0.391]	0.027 [-0.027, 0.080]	0.004 [-0.049, 0.058]
Melbourne	0.311* [0.248, 0.372]	-0.113* [-0.180, -0.045]	0.248* [0.182, 0.311]	0.073* [0.005, 0.141]	0.287* [0.223, 0.349]	**1.000**	0.074* [0.021, 0.127]	0.203* [0.151, 0.254]
Perth	-0.016 [-0.084, 0.053]	0.035 -0.033, 0.104]	-0.083* [-0.150, -0.015]	0.001 [-0.067, 0.069]	-0.084* [0.016, 0.151]	-0.100* [-0.167, -0.031]	**1.000**	0.126* [0.073, 0.179]
Sydney	0.035 [-0.033, 0.104]	0.157* [0.090, 0.223]	0.512* [0.460, 0.560]	0.060 [-0.009, 0.128]	0.084* [0.016, 0.151]	0.069* [0.000, 0.136]	-0.013 [-0.081, 0.056]	**1.000**

Note: The upper half (shaded) is for PM_{10} and the lower half is for $PM_{2.5}$. Values in brackets are the confidence intervals. * indicates p<0.05.

Table S3. Membership degrees matrix after Fuzzy c-means clustering.

City	***Cluster 1***	***Cluster 2***	***Cluster 3***	***Cluster 4***	***Cluster 5***	***Cluster 6***
	PM_{10}					
Adelaide	0.00952	0.00729	0.01234	0.00646	**0.95225**	0.01214
Brisbane	0.00283	0.00219	0.00354	0.00169	0.00321	**0.98654**
Canberra	0.00207	**0.98863**	0.00245	0.00138	0.00258	0.00288
Darwin	0.00019	0.00013	0.00019	**0.99908**	0.00021	0.00021
Hobart	0.10615	**0.23992**	0.17802	0.08517	0.20507	0.18567
Melbourne	0.13742	0.12085	0.16631	0.08210	**0.33170**	0.16162
Perth	0.00234	0.00179	**0.98777**	0.00153	0.00315	0.00341
Sydney	**0.99605**	0.00057	0.00088	0.00056	0.00092	0.00102
	***Dunn's Fuzziness Coefficient*: 0.777**			***BSS/TSS*: 0.864**		
	$PM_{2.5}$					
Adelaide	**0.97273**	0.00776	0.00447	0.00609	0.00311	0.00584
Brisbane	0.00382	0.00293	0.00283	0.00369	0.00231	**0.98442**
Canberra	0.00211	0.00210	**0.98982**	0.00255	0.00137	0.00205
Darwin	0.00054	0.00052	0.00050	0.00051	**0.99732**	0.00061
Hobart	0.17165	0.17898	**0.19542**	0.13957	0.12797	0.18641
Melbourne	0.00368	**0.98823**	0.00214	0.00231	0.00146	0.00217
Perth	**0.26200**	0.15533	0.11985	0.17120	0.09779	0.19383
Sydney	0.00235	0.00186	0.00209	**0.99034**	0.00116	0.00219
	***Dunn's Fuzziness Coefficient*: 0.775**			***BSS/TSS*: 0.796**		